SIMULATION OF FUZZY BASED DIRECT TORQUE CONTROL OF INDUCTION MOTOR DRIVE

A DISSERTATION

Submitted in partial fulfillment of the requirements for the award of the degree of

MASTER OF TECHNOLOGY

in

ELECTRICAL ENGINEERING

(With Specialization in Power Apparatus & Electric Drives)

By

SUDHAKAR KAMMILI

DEPARTMENT OF ELECTRICAL ENGINEERING
INDIAN INSTITUTE OF TECHNOLOGY ROORKEE
ROORKEE - 247 667 (INDIA)

JUNE, 2008

I.D. No.-M.T 439 / 2008-23 SP

CANDIDATE'S DECLARATION

I hereby declare that the work that is being presented in this dissertation report entitled **"SIMULATION OF FUZZY BASED DIRECT TORQUE CONTROL OF INDUCTION MOTOR DRIVE"** submitted in partial fulfillment of the requirements for the award of the degree of **Master Of Technology** with specialization in **Power Apparatus and Electric Drives,** to the **Department Of Electrical Engineering, Indian Institute Of Technology, Roorkee**, is an authentic record of my own work carried out, under the guidance of **Dr. S.P.Singh**, Professor, Department of Electrical Engineering.

The matter embodied in this dissertation report has not been submitted by me for the award of any other degree or diploma.

Date: 26-6-08
Place: Roorkee

K. Sudhakar
Sudhakar Kammili

This is to certify that the above statement made by the candidate is correct to the best of my knowledge.

26/6/08

Dr. S.P.Singh
Professor
Department of Electrical Engineering
Indian Institute of Technology
ROORKEE – 247 667
INDIA.

ACKNOWLEDGEMENT

I wish to express my deep sense of gratitude and sincere thanks to my guide Dr.S.P.Singh, Professor, Department of Electrical Engineering, IIT Roorkee for being helpful and a great source of inspiration. His keen interest and constant encouragement gave me the confidence to complete my work. I wish to extend my sincere thanks for his excellent guidance and suggestions in spite of his hectic schedule for the successful completion of my project work.

I am indebted to all my classmates from Power Apparatus & Electric Drives group for taking interest in discussing my problems and encouraging me. Thanks are also due to those who helped me directly or indirectly in my endeavor.

I'm highly indebted to my parents and family members, whose sincere prayers, best wishes, moral support and encouragement have a constant source of assurance, guidance, strength, and inspiration to me.

(SUDHAKAR KAMMILI)

ABSTRACT

The control and estimation of ac drives in general are considerably more complex than those of dc drives, and this complexity increases substantially if high performances are demanded In recent years, the application field of Direct Torque Control (DTC), a variation of vector control, of induction machines has greatly increased in the areas of the traction, paper and steel Industry, and so on.

Direct Torque Control is one of the actively researched control schemes, which is based on the decoupled control of flux and torque providing a very quick and robust response with a simple control construction in ac drives. The main limitations of the conventional DTC are large torque and current ripples and variable switching frequency. These disadvantages can be overcome by using Fuzzy Space Vector Modulation (FSVM).

Direct Torque Control of Induction Motor using Fuzzy based SVM has been adopted for the present study. The torque ripple and Flux error can be reduced by using Fuzzy based SVM as compared to classical DTC. In present work, these comparative features have been highlighted, through MATLAB simulation.

CONTENTS

	Page No.
CANDIDATES DECLARATION	i
ACKNOWLEDGEMENT	ii
ABSTRACT	iii
CONTENTS	iv
LIST OF FIGURES	vii
LIST OF TABLES	ix
CHAPTER 1: INTRODUCTION	
1.1 Overview	1
1.2 Scalar control	3
1.3 Vector or field oriented Control	3
1.4 Direct Torque and Flux Control	3
1.4.1 Main features of the DTC	4
1.4.2 Advantages of the DTC	4
1.4.3 Main Disadvantages of Convectional DTC	4
1.5 Literature Review	4
1.6 Report Organization	6
CHAPTER 2: BASIC THEORYOF DIRECT TORQUE CONTROL	
2.1 Introduction	7
2.2 Fundamentals to Produce Fast Torque Response	7
2.3 Basic Direct Torque Control Strategy	9
2.3.1 Flux and Torque Comparators	9
2.3.2 Voltage Source Inverter	10
2.3.3 Stator Flux-linkage Space Vector Control	10
2.3.4 Selection Table for Direct Torque Control	12
2.3.5 Stator Flux-linkage Space Vector Position Estimation	14
2.3.6 Electromagnetic Torque and Stator Flux-linkage Estimator	14

CHAPTER 3: SPACE VECTOR MODULATION AND FUZZY LOGIC THEORY

3.1 General 15

3.2 Space Vector Modulation 16

3.2.1 Space Vector 16

3.2.2 Three phase to two phase transformation 19

3.2.3 Estimation of T_1,T_2, and T_0 20

3.2.4 Generalized formulas to any Sector 21

3.3 Principles of Fuzzy logic 21

3.3.1 Introduction 21

3.4 Structure of Fuzzy Controller 22

3.5 Advantages of Fuzzy 24

CHAPTER 4: DIRECT TORQUE CONTROL OF INDUCTION MOTOR USING FUZZY SPACE VECTOR MODULATION TECHNIQUE

4.1 DTC of Induction motor using voltage vector reference based SVM 26

4.2 Speed Controller, Flux Controller, Torque Controller 27

4.3 Space Vector Modulation 27

4.4 Voltage Source Inverter 28

4.5 Induction Motor 28

4.6 Flux and Torque Estimator 32

4.7 Modeling of DTC using Voltage Vector based SVM 33

4.7.1 Axis Transformation ($e^{j\theta}$) 33

4.7.2 Space Vector Modulation 33

4.7.3 Voltage Source Inverter 35

4.7.4 Induction Machine Model 36

4.7.5 Flux and Torque Estimation 37

4.8 DTC of Induction motor using Stator flux error Vector based SVM

4.8.1 General 37

4.8.2 Description of the control scheme 37

4.8.3 Speed Controller and Torque Controller 40

4.8.4 Modeling of DTC using Fluzzy based SVM 41
A. Complete model of Direct Torque Control of Induction motor using Flux Error Vector based Space Vector Modulation 41

CHAPTER 5: SIMULATION RESULTS 42

5.1 Simulation Results of DTC of Induction Motor using Fuzzy based SVM technique 42
5.2 Comparisons with Classical DTC of Induction motor 49

CHAPTER 6: CONCLUSIONS AND FUTURE SCOPE 51

References 52

Appendix 55

List of Figures

Chapter 2

2.1 Stator flux-linkage and Stator current space vectors 8
2.2 Stator flux based DTC induction motor Drive with VSI. 9
2.3 PWM VSI 10
2.4 Stator flux vector locus and different possible switching voltage vectors 11

Chapter 3

3.1 Representation of Rotating Vector in Complex Plane 18
3.2 Voltage Space Vector and its components in (d,q) 19
3.3 Reference vector as a combination of adjacent vectors at sector 1 20
3.4 Blocks of a Fuzzy Controller 22

Chapter 4

4.1 The Complete Block diagram of SVM based DTC induction motor drive 27
4.2 A cross view of a three-phase induction motor 28
4.3 Simulink block of the axis transformation· 33
4.4 Simulink block of the SVM and V.S.I 34
4.5 Simulink model of an Induction machine 35
4.6 Simulink block of the Flux and Torque Estimator. 36
4.7 The complete block diagram of DTC of IM using fuzzy based SVM. 37
4.8 Space voltage vector and stator flux vector in stationary Reference frame. 38
4.9 Membership functions of flux error e_{ψ},torque error e_t and angle η 39
4.10 Simulink model of DTC of IM using Fuzzy Based SVM 41

Chapter 5

5.1 phase voltages Va Vb, Vc (volts) Vs time(sec) 42
5.2 line current of the induction motor for classical DTC. 66
5.3 stator flux linkage with respect to time for classical DTC 43
5.4 Speed and torque response of the induction motor for classical DTC 44

5.5	Phase voltages Va Vb, Vc (volts) Vs time(sec)	45
5.6	Three phase currents of the Induction Motor with fuzzy svm	46
5.7	d-q components of Stator current Vs time	46
5.8	Speed and torque response of the induction motor at rated speed and rated torque	47
5.9	Stator flux linkage with respect to time in fuzzy DTC	47
5.10	Stator Current For Fuzzy DTC	48
5.11	(a) Stator flux linkage with respect to time in classical DTC	49
	(b) Stator flux linkage with respect to time with fuzzy DTC	49
5.12	(a) Electromagnetic torque with respect to time in classical DTC	50
	(b) Electromagnetic torque with respect to time in Fuzzy DTC	50

List of Tables

Chapter 2

2.1 General Selection Table for Direct Torque Control 13

2.2 Look up table for Direct Torque Control 14

Chapter 3

3.1 Switch States for Three Phase Voltage Source Inverter (VSI) 18

Chapter 4

4.1 Fuzzy Rule Base for 16 Rules 39

Chapter-1

INTRODUCTION

1.1 Overview

The history of electrical motors goes back as far as 1820, when Hans Christian Oersted discovered the magnetic effect of an electric current. One year later, Michael Faraday discovered the electromagnetic rotation and built the first primitive D.C. motor. Faraday went on to discover electromagnetic induction in 1831, but it was not until 1883 that Tesla invented the A.C asynchronous motor. Currently, the main types of electric motors are still the same, DC, AC asynchronous and synchronous, all based on Oersted, Faraday and Tesla's theories developed and discovered more than a hundred years ago.

Drives used in machine tools, spindles, high speed elevators, dynamometers, mine wonders, rolling mills, and glass float lines. Such high performance applications require a high speed holding accuracy, a wide range speed control, and fast transient response. Until recently, such drives have almost exclusively been the domain of d.c. motors combined with various configurations of a.c./d.c. converters depending upon the application.

In the past, d.c. motors were used extensively in areas where variable-speed operation was required, since their flux and torque could be easily controlled by field and armature currents. Variable D.C. drives were widely used because of the easy of control and versatility of the dc separately excited motor. However dc motors have certain disadvantages because they require periodic maintenance due to the existence of the commutator and the brushes and they can not be used in explosive or corrosive environments and they have limited commutator capabilities under high speed, high voltage operational conditions. These problems can be overcome by the application of a.c. motors, which can have simple and rugged structure, high maintainability and economy. They are robust and immune to heavy overloading. Among the various a.c. drive systems, the cage induction motor have a particular cost advantage that means it is available at all power ratings at lower cost.

The control of a.c. drives is more difficult because, in ac machines, both the phase angle and the modules of the current have to be controlled, or in other words the current vector has to be controlled. This technique is well known vector control technique. In the same way in Direct Torque Control, it can be possible to control the induction machine by controlling the variables of the voltage vector that means by controlling the phase and modules of the voltage vector, the control of a.c. machine is achieved. But in d.c. machines, the orientation of the field flux and armature m.m.f is fixed by the commutator and the brushes, while in a.c. machines the field flux and the spatial angle of the armature m.m.f require external control. In the absence of this control, the spatial angles between the various fields in a.c. machines vary with the load and results into unwanted oscillating dynamic response.

Before the days of power electronics, a limited speed control of induction motor was achieved by switching the three-stator windings from delta connection to star connection, allowing the voltage at the motor windings to be reduced. Induction motors are also available with more than three stator windings to allow a change of the number of pole pairs. However, a motor with several windings is more expensive because more than three connections to the motor are needed and only certain discrete speeds are available. Another alternative method of speed control can be realized by means of a wound rotor induction motor, where the rotor winding ends are brought out to slip rings. However, this method obviously removes most of the advantages of induction motors and it also introduces additional losses. By connecting resistors or reactance in series with the stator windings of the induction motors, poor performance is achieved.

With the enormous advances made in semiconductor technology during the last two decades, the required conditions for developing a proper induction motor drive are present. These conditions can be divided mainly in two groups:

- The decreasing cost and improved performance in power electronic switching devices.
- The possibility of implementing complex algorithms in the new microprocessors.

The different control techniques of Induction Motor Drives are

1 Scalar control
2 Vector or field-oriented control
3 Direct torque and flux control

1.2 Scalar control

Scalar control, as the name indicates, is due to magnitude variation of the control variables only, and discards the coupling effect (i.e., both torque and flux are functions of voltage or current and frequency) in the machine.. Scalar-controlled drives have been widely used in industry. However, their importance has diminished recently because of the superior performance of vector controlled drives, which is demanded in many applications.

1.3 Vector or field oriented Control

The invention of vector control in the beginning of 1970s, and the demonstration that an induction motor can be controlled like a separately excited dc motor, brought a renaissance in the high performance control of ac drives. Because of dc machine-like performance, vector control is also known as decoupling, orthogonal control. Vector control is applicable to both induction and synchronous motor drives. Vector control, are complex and the use of powerful microcomputer or DSP is mandatory. It appears that eventually, vector control will outs scalar control, and will be accepted as the industry-standard control of ac drives.

1.4 Direct Torque and Flux Control

DTC-based drives selects the inverter switching states using the inverter-switching table, neither current controllers nor pulse-width modulation(PWM) modulator is required, thereby providing fast torque response[7]. However, this switching-table-based DTC approach is accompanied by some disadvantages, which are overcame by space vector modulation technique.

1.4.1 Main Features of the DTC:

1. Direct control of flux and torque
2. Indirect control of stator currents and voltages
3. Stator fluxes and voltages are approximately sinusoidal
4. Possibility of reduced torque oscillations
5. High dynamic performance

1.4.2 Advantages of DTC:

1. Absence of coordinate transformations
2. Absence of separate voltage modulation block
3. Absence of voltage decoupling circuits
4. Absence of several controllers
5. Only the sector where the flux-linkage space vector is located, and not the actual flux-linkage space vector-position, has to be determined
6. Minimal torque response time

1.4.3 Main Disadvantages of Convectional DTC:

1. Requirement for flux and torque estimators
2. Changing switching frequency
3. Torque ripple is high

1.5 Literature Review

In 1971 F. Blaschke presented the first paper on field-oriented control (FOC) for induction motors. Since that time, the technique was completely developed and today is mature from the industrial point of view. Today field oriented controlled drives are an industrial reality and are available on the market by several producers and with different solutions and performance. Thirteen years later, a new technique for the torque control of induction motors was developed and presented by I. Takahashi as direct torque control (DTC) (1985) [1], and by M. Depenbrock as direct self control (DSC) [2]. FOC and DTC schemes are compared in terms of torque and current ripples by Domenico Casadei.

Different direct torque control strategies like classical DTC, SVM DTC were discussed by P. Marino in 2001[21].

Since the beginning, the new technique was characterized by simplicity, good performance and robustness. Using DTC or DSC it is possible to obtain a good dynamic control of the torque without any mechanical transducers on the machine shaft. In 1989 I.Takahashi and Y. Ohmori [3] presented High-performance Direct Torque control of Induction motor. They have been carried out simulations and experiments to verify the feasibility of the following priorities; 1) high speed torque control, 2) regulation of the primary flux, 3) decreasing the zero phase sequence currents, minimization of the inverter switching frequency.

In 1991 Thomas G. Habetler, Francesco Profumo, Michele pastrorelli and Leon M. Tolbert [4] proposed Direct Torque Control of Induction Machines by space vector modulation technique. They described a control scheme for direct torque and flux control of induction machines based on the stator-flux-field orientation method. With the proposed predictive control scheme, an inverter duty cycle has directly calculated each fixed switching period based on the torque and flux errors and they also proposed a method by which a voltage space vector can be calculated using the space vector PWM technique.

In 1994 D.Casadei, G.Grandi, G.Serra and A.Tani [5]. are investigated the influence of the amplitude of the flux and torque hysteresis bands on switching frequency in direct torque control. In 1997 S.Chakrabarthi, M.Ramamoorty and V.R Kanetkar [10] have developed a simulation program for Reduction of torque ripple in DTC of induction motor drives using space vector modulation based pulse width modulation. Arias; J.L. Romeral, E. Aldabas presented DTC scheme with two fuzzy logic controllers, in which one of them used for calculating duty ratio and the other to calculate change in duty ratio in "Fuzzy Logic Direct Torque Control" 2000 [22]

In 2005 Lin Chen, Kang-Ling Fang, and Zi-fan hu [11] introduced A Scheme of Fuzzy DTC for Induction Motor Drive. A.Tripathi, A.M. Kkambadkone and S K Panda (in 2001) [12] presented Space vector based, Constant Frequency and dead beat Stator Flux Control of AC machines. In the proposed control scheme, the switching information is obtained directly from the error in flux. In 2004 Nik Rumzi Nik Idris and Abdul Halim

Mohamed Yatim [6] have done work on DTC of induction machines with constant frequency and reduced torque ripple.

1.7 Report Organization

In chapter 1, there is a brief introduction about the control methods of the induction motor, like Scalar, Vector and Direct torque and flux control methods.

In chapter 2, the principle of direct torque controlled induction motor drive, supplied by a voltage source inverter is explained. The method to control directly the stator flux linkage and electromagnetic torque by the selection of the optimum inverter switching modes and the selection made to restrict the flux and torque errors within respective flux and torque hysteresis bands, to obtain fast torque response, low inverter switching frequency, and low harmonic losses etc is explained.

In chapter 3, SV PWM technique for three phase voltage source inverters is discussed. The switching time period for the space vector PWM is derived. Fuzzy logic theory is also discussed.

In chapter 4, the implementation of the Direct Torque Control of Induction motor using fuzzy space vector modulation technique is explained in detail with Block Diagrams and modeling of the control strategy are also shown. An induction motor load is connected and different waveforms are obtained by simulating the model.

In chapter 5, the simulated results, that are the waveforms of the current, motor speed, torque, angle for sector determination, phase voltage waveforms etc. are shown for different load torques and speed references.

In chapter 6, the entire work that has been taken up in the dissertation has been discussed with a view to future scope of the subject by expanding the boundaries or limitations.

Chapter-2

BASIC THEORY OF DIRECT TORQUE CONTROL

2.1 Introduction

Induction motors are characterized by complex, nonlinear, time-varying dynamics and inaccessibility of some states and outputs for measurements. In field oriented control (FOC) of induction motor, stator current is divided into torque and flux producing components. These components are controlled in a fashion similar to that of a separately excited dc motor. Because of the transformations, this method is complex. To simplify the control strategy, in 1985, the DTC was introduced by Depenbrock. In conventional DTC optimum voltage vector is selected from the switching table based on the flux and torque errors. As this method does not involve with any transformations, this method was widely used in Industrial applications.

2.2 Principles of Direct Torque Control

In stationary reference frame, space voltage vectors of both stator and rotor of the machine are represented as follows in eq 1&2.

$$\overline{V}_s = r_s i_s + d\psi_s/dt \qquad (2.1)$$

$$Vr = r_r i_r + d\psi_r/dt - j\omega\psi_r \qquad (2.2)$$

Where r_s and r_r are stator and rotor resistances, us and u r are stator and rotor space voltage vectors, ψ_s and ψ_r are stator and rotor flux respectively. ω is the angular speed of the rotor. The torque could be expressed in terms of stator flux, rotor flux and the angle γ between stator flux and rotor flux.

The stator flux-linkage space vector is

$$\psi_s = \int (V_s - r_s i_s)\,dt \qquad (2.3)$$

From equation (2.3), if the stator ohmic drops can be neglected, then the equation (2.3) can be modified as shown below

$$d\psi_s / dt = \overline{V}_s \qquad (2.4)$$

From the equation (2.4), in a short Δt time, when the voltage vector is applied,

$\Delta\psi_s = \overline{V}_s.\Delta t$, that means the stator flux-linkage moves by $\Delta\overline{\psi_s}$ in the direction of stator-voltage space vector at a speed which proportional to the magnitude of the stator-voltage space vector (which is proportional to the d.c. voltage).

The electromagnetic torque in the three phase induction machines can be estimated as follows [ ]

$$T_e = \frac{3}{2} P \frac{L_m}{L_s' L_r} |\overline{\psi}_r| . |\overline{\psi}_s| . \sin\gamma \qquad (2.5)$$

where γ is the angle between the stator and rotor flux linkage space vectors.

$$T_e \alpha \psi_s \psi_r \sin\gamma \qquad (2.6)$$

$\overline{\psi_s}$ is the stator flux linkage space vector and ψ_r is the rotor flux linkage space vector (both fixed to the stationary reference frame fixed to the stator) From the above equation, if the stator and rotor flux linkages are assumed to be constant, the electromagnetic torque can be changed by changing γ in the required direction. γ can be easily changed by switching on the appropriate stator-voltage space vectors.

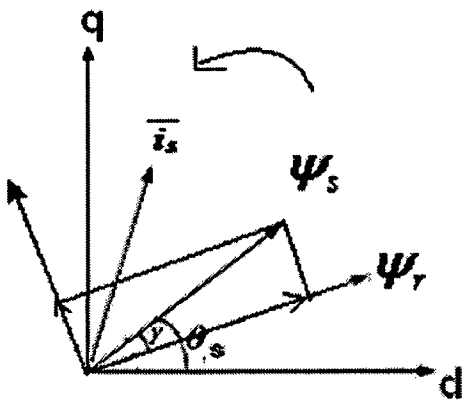

Fig. 2.1. Stator flux-linkage and Stator current space vectors.

2.3 Basic Direct Torque Control Strategy

The control block diagram of the stator flux based DTC induction motor drive with VSI is shown in Fig 2.2.The control block is composed of Flux comparator, Torque comparator, Inverter optimum switching table, Electromagnetic torque and Stator flux-linkage estimator and Voltage source inverter. Brief explanation about these blocks is here.

2.3.1 Flux and Torque Comparators

In Fig. 2.2 the reference value of the stator flux-linkage space vector modulus, $|\overline{\psi}_{ref}|$, is compared with the actual modulus of the stator flux-linkage space vector, $|\overline{\psi}_s|$, and the resulting error is fed into the two-level stator flux hysteresis comparator. Similarly the reference value of the electromagnetic torque, T_{eref}, is compared with the actual electromagnetic torque , T_e, and the resulting torque error is fed into the three-level torque hysteresis comparator.

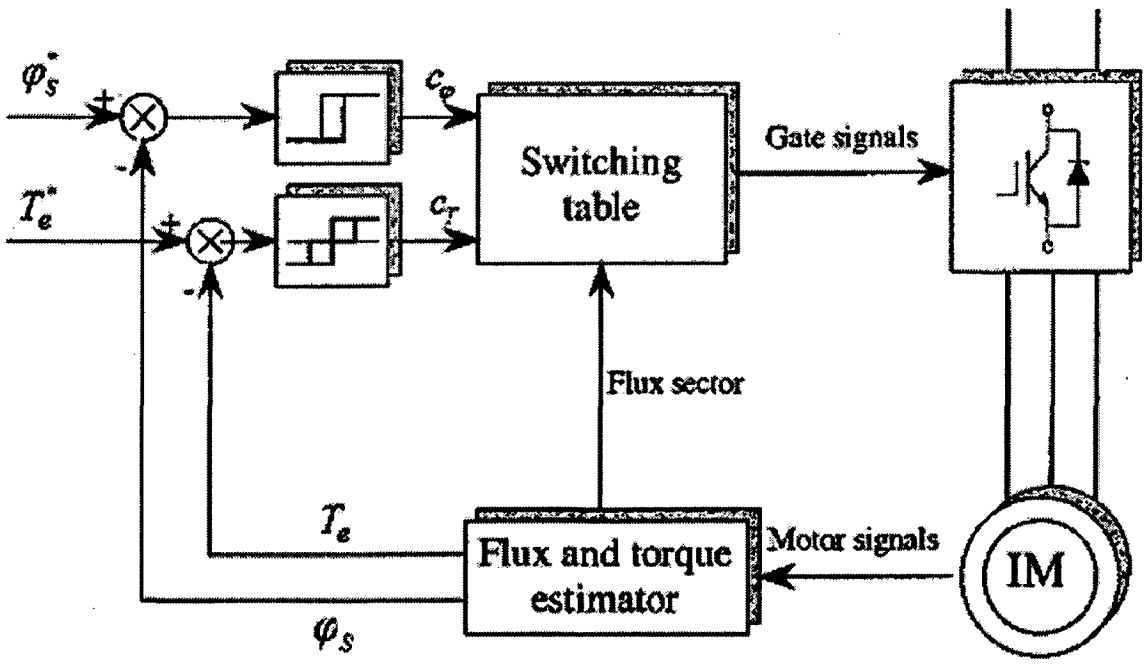

Fig.2.2. Stator flux based DTC induction motor Drive with VSI

2.3.2 Voltage Source Inverter

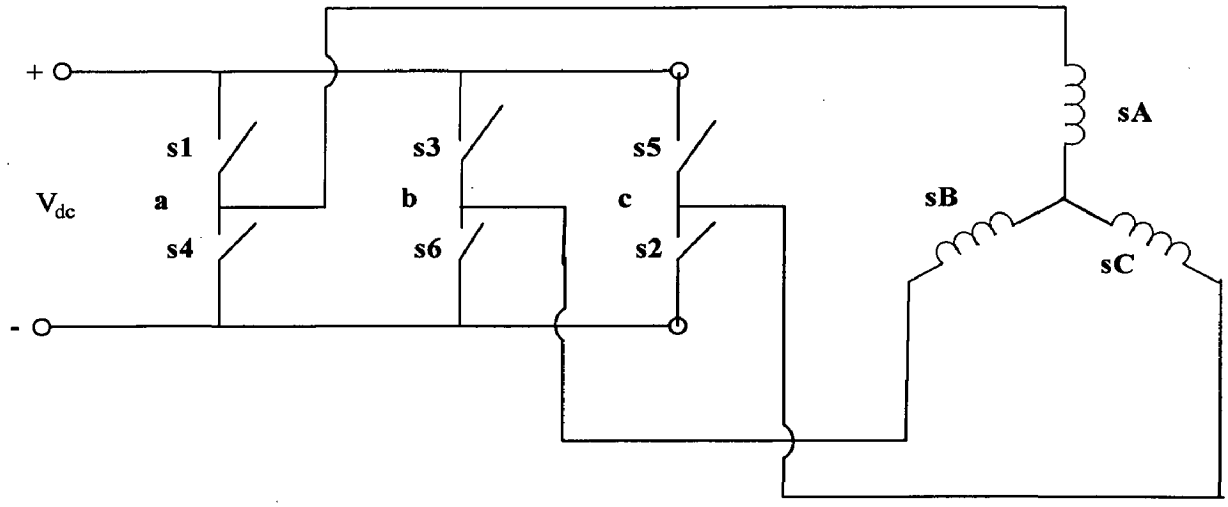

Fig 2.3 PWM VSI

By considering the six-pulse VSI, there are six non zero active voltage-switching space vectors ($\overline{v_1}, \overline{v_2}, \ldots \overline{v_6}$) and two non space vectors ($\overline{v_7}, \overline{v_8}$). These are shown in Fig 2.3. The six active inverter-switching vectors can be expressed as [7]

$$\overline{v_s} = \overline{v_k} = \frac{2}{3} V_{dc} \exp[j\{k-1)\pi/3] \qquad \text{k=1, 2, 3,..., 6} \qquad (2.6)$$

where V_{dc} is the d.c. link voltage. For k=7, 8, $\overline{v_k} = 0$ holds for the two zero switching states where the stator windings are short circuited, $\overline{v_s} = \overline{v_k} = 0$.

2.3.3 Stator Flux-linkage Space Vector Control

Figure 2.4 shows the possible dynamic locus of the stator flux, and its different variation depending on the VSI states chosen. The possible global locus is divided into six different sectors signaled by the discontinuous line.

From the equation (2.5), the stator flux linkage space vector will move fast if non-zero switching vectors are applied, for a zero vector it will almost stop (it will move very slowly due to the small ohmic voltage drop). In the DTC drive, at every sampling period, the switching vectors are selected such that the stator flux-linkage error and torque errors should be confined with in the respective hysteresis bands. The drive may lose the

control, if the width of the hysteresis bands is too small value. It is assumed that the widths of these hysteresis bands are $2\Delta\overline{\psi_s}$ and $2\Delta T_e$ respectively [1].

If the selected switching vector is zero, then the speed of the stator flux-linkage space vector is zero, which can be changed by changing the output ratio between the zero and non-zero voltage vectors and the duration of the zero states has a direct effect on the electromagnetic torque oscillations. If a reduced stator flux-linkage space vector is required, it can be achieved by applying switching voltage vectors which are directed towards the centre of the rotor, and if an increased stator flux-linkage space vector is required, it can be achieved by applying switching voltage vectors which are directed out from the centre of the rotor, which is shown in Fig. 2.4. To keep the modulus of the stator flux linkage space vector ($|\overline{\psi_s}|$) within the hysteresis band, whose width is $2\Delta\overline{\psi_s}$. The locus of the flux linkage space vector is divided into several sectors, and due to the six step inverter, the minimum number of sectors required is six. The sectors are also shown in Fig 2.3 as dotted lines [7].

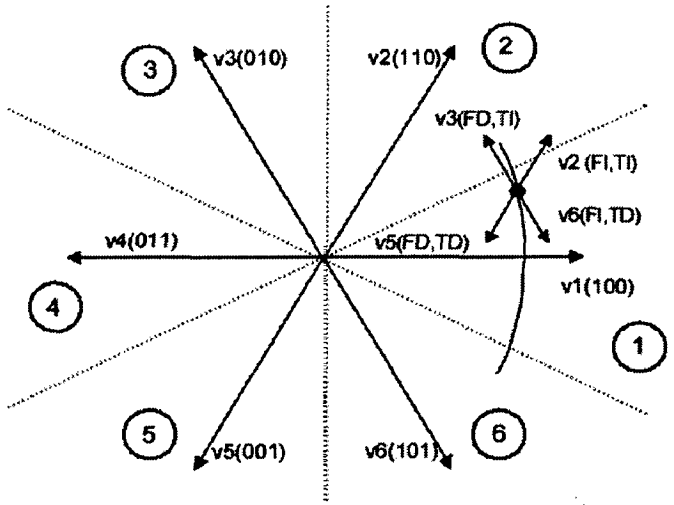

Fig 2.4 Stator flux vector locus and different possible switching voltage vectors.
FD: flux decrease. FI: flux increase. TD: torque decrease. TI: torque increase

There are eight switching vectors to keep the modulus of the stator flux linkage space vector ($|\overline{\psi_s}|$) within the hysteresis band. It is assumed that initially the stator flux-linkage space vector is at position P_0, thus in sector1. Assuming that the stator flux-linkage space vector is rotating in anticlockwise, if the stator flux-linkage space vector is

at the upper limit ($|\overline{\psi}_{sref}| + \Delta\overline{\psi}_s$) so it must be reduced. This can be achieved by applying the suitable switching vector $\bar{v}_3$, as shown in Fig. 2.4. Thus the stator flux-linkage space vector will move rapidly from sector 1 to the sector 2. At this point the stator flux-linkage space vector is again at its upper limit, it has to be reduced when it is rotated in anti clockwise, hence for this purpose the switching vector $\bar{v}_4$ has to be selected.

On the other hand, if the stator flux-linkage space vector moves in the clockwise direction, then the switching vector $\bar{v}_5$ would have to be selected, since this would ensure the required rotation and also the required flux decrease.

2.3.4 Selection Table for Direct Torque Control

In Accordance with figure 2.4, the general table 2.1 can be written. It can be seen from table 2.1, that the states V_k and V_{k+3}, are not considered in the torque because they can both increase (first 30 degrees) or decrease (second 30 degrees) the torque at the same sector depending on the stator flux position. The usage of these states for controlling the torque , dividing the total locus into twelve sectors instead of just six

VOLTAGE VECTOR	INCREASE	DECREASE
Stator Flux	V_k, V_{k+1}, V_{k-1}	$V_{k+2}, V_{k-2}, V_{k+3}$
Torque	V_{k+1}, V_{k+2}	V_{k-1}, V_{k-2}

Table 2.1: General Selection Table for Direct Torque Control, being "k" the sector number.

The digital output signals of a two level flux hysteresis comparator are

$d\psi = 1$ if $|\overline{\psi}_s| \leq |\overline{\psi}_{sref}| - |\Delta\psi_s|$, $d\psi = 1$ means a stator flux increase is required.(FI)

$d\psi = 0$ if $|\overline{\psi}_s| \geq |\overline{\psi}_{sref}| + |\Delta\psi_s|$, $d\psi = 1$ means a stator flux decrease is required.(FD)

The digital output signals of a three level hysteresis comparator are

- For the stator flux-linkage space vector rotates in the forward direction (anti clockwise direction)

dt_e =1 if $|t_e| \leq |t_{eref}| - |\Delta t_e|$ means if a torque increase is required (TD)

dt_e =0 if $t_e \geq t_{eref}$ means if no change in the torque is required (T=)

- For the stator flux-linkage space vector rotates in the reverse direction (clockwise direction)

dt_e = -1 if $|t_e| \geq |t_{eref}| + |\Delta t_e|$ means if a torque decrease is required (TD)

dt_e =0 if $t_e \leq t_{eref}$ means if no change in the torque is required(T=)

Finally, the DTC classical look up table is as follows:

Table 2.2. Look up table for Direct Torque Control. FD /FI: flux decrease/increase.TD/=/I:torquedecrease/equal/increase. S_x: stator flux sector. Φ: stator flux modulus error after the hysteresis block. τ: torque error after the hysteresis block.

ψ	T_e	S_1	S_2	S_3	S_4	S_5	S_6
FI	TI	V_2	V_3	V_4	V_5	V_6	V_1
	T=	V_0	V_7	V_0	V_7	V_0	V_7
	TD	V_6	V_1	V_2	V_3	V_4	V_5
FD	TI	V_3	V_4	V_5	V_6	V_1	V_2
	T=	V_7	V_0	V_7	V_0	V_7	V_0
	TD	V_5	V_6	V_1	V_2	V_3	V_4

Table 2.2. Look up table for Direct Torque Control. FD /FI: flux decrease/increase.TD/=/I:torquedecrease/equal/increase. S_x: stator flux sector. Φ: stator flux modulus error after the hysteresis block. τ: torque error after the hysteresis block.

The sectors of the stator flux space vector are determined from $S_1$to S_6. Stator flux modulus error after the hysteresis block (ψ) can take three different values .The zero

voltage vectors V_0 and V_7 are selected when the torque error is with in the given hysteresis limits and must remain unchanged.

2.3.5 Stator Flux-linkage Space Vector Position Estimation

The position of the stator flux-linkage space vector that means stator flux angle (θ_s) can be determined by using the estimated values of the direct and quadrature-axis stator flux-linkages in the stationary reference frame (ψ_{sD}, ψ_{sQ}), thus

The stator flux angle (θ_s) is [7]

$$\theta_s = \tan^{-1}(\psi_{sQ}/\psi_{sD}) \tag{2.7}$$

2.3.6 Electromagnetic Torque and Stator Flux-linkage Estimator

The stator flux linkage space vector is [7]

$$\overline{\psi}_s = \int(\overline{v_s} - R_s\overline{i_s})dt \tag{2.8}$$

Where $\overline{\psi}_s = \psi_{sD} + j\psi_{sQ}$, $\overline{v_s} = v_{sD} + jv_{sQ}$ and $\overline{i_s} = i_{sD} + ji_{sQ}$

$$\psi_{sD} = \int(v_{sD} - R_s i_{sD})dt \tag{2.9}$$

$$\psi_{sQ} = \int(v_{sQ} - R_s i_{sQ})dt \tag{2.10}$$

Where $\psi_{sD}, v_{sD}, i_{sD}$ and ψ_{sQ}, v_{sQ}, i_{sQ} are the d-axis and q-axis quantities of stator flux-linkage space vector, stator voltage space vector and stator current space vector components respectively.

Chapter 3

SPACE VECTOR MODULATION AND FUZZY LOGIC THEORY

3.1 General

Voltage-source inverters have evolved as the most preferred power conversion method for ac drive applications. Hard switching techniques continue to dominate the market, ranging from applications at low power using MOSFET semiconductor switches, through the medium power range, which is the domain of bipolar Darlington transistor and the IGBT, up to GTO inverters which are applied at megawatt power level. Typical applications are motion control systems, industrial drives, and high-power ac traction equipment. Although very different in nature, these schemes rely on a common basic technology: pulse width modulation [19].

Research in this field has been very progressive during the past decades. Apparently, this process has not yet come to a state of saturation, as novel PWM methods continue to emerge. It appears, though, that one important aspect of pulse width modulation techniques has been given little attention so far: pulse width control in the range of over modulation.

Pulse width modulation method employs a triangular carrier wave modulated by a sine wave and the points of intersection determine the switching points of the power devices in the inverter. However, this method is unable to make full use of the inverter's supply voltage and the asymmetrical nature of the PWM switching characteristics produces relatively high harmonic distortion in the supply. Many different PWM methods have been developed to achieve the following aims: wide linear modulation range; less switching waveform; less total harmonic distortion (THD) in the spectrum of switching waveform; and easy implementation and less computation time. For a long period, carrier based PWM methods were widely used in most applications. A more advanced algorithm like Space Vector Modulation overcomes the drawbacks of the Sine PWM algorithm and increases the overall system efficiency. Space Vector PWM(SVPWM) is more sophisticated technique for generating a fundamental sine wave that provides a higher voltage to the motor and lower total harmonic distortion.

3.2 Space Vector Modulation

Pulse Width Modulation and Space Vector Modulation are two popular techniques for providing control of inverter drives. Space Vector Modulation (SVM) Technique has become the most popular and important PWM technique for three phases Voltage Source Inverters for the control of AC Induction, Brushless DC, Switched Reluctance and Permanent Magnet Synchronous Motors. It is a more sophisticated technique for generating sine wave that provides a higher voltage to the motor with lower total harmonic distortion. It confines space vectors to be applied according to the region where the output voltage vector is located.The SVM technique is more popular because of its excellent features: wide linear modulation range; output voltage is $2/\sqrt{3}$ as larger as the conventional sinusoidal modulation; More efficient use of DC supply voltage; Advanced and computation intensive PWM technique; Higher efficiency; Prevent un-necessary switching hence less commutation losses; A different approach to PWM modulation based on space vector representation of the voltages in the $\alpha - \beta$ plane [29].

3.2.1 Space Vector

The concept of space vector is derived from the rotating field of AC machine which is used for modulating the inverter output voltage. In this modulation technique the three phase quantities can be transformed to their equivalent 2-phase quantity using parks transformation. From this two-phase component the reference vector magnitude can be found and used for modulating the inverter output.

A three-phase inverter can assume eight different switching states, corresponding to seven discrete voltage vectors at the output (Fig.3.1). The PWM strategy defines the sequencing of the available vectors in such a way that the average voltage within one cycle corresponds to the reference The cycle time T_S is defined as the time necessary to go through the sequence of three successive vectors . The cycle T_S can also be defined as the minimum interval where the average inverter output corresponds to the reference u^* .The space vector modulation and the problem of selecting the appropriate switching sequence is best understood if the phase quantities are transformed into the $\alpha - \beta$ stationary reference frame [30]

$$u_\alpha = u_a - (u_b + u_c)/2 \qquad (3.1)$$

$$u_\beta = -\frac{\sqrt{3}}{2}(u_b + u_c) \qquad (3.2)$$

(u_a,u_b, and u_c are the phase voltages, u_α and u_β are the components of the voltage vector $\bar{u}_{\alpha\beta}$, axes α is aligned with the motor phase A winding)

Table I gives the α and β components of each voltage vector, together with the switching states for all six segments defined in Fig.3.1.

State	State No.	Switch States	V_{ab}	V_{bc}	V_{ca}	Space Vector
S1,S2,S6 are on S4,S5,S3 are off	1	100	V_{dc}	0	$-V_{dc}$	$u_1 = 1 + j0.577$
S2,S3,S1 are on S5,S6,S4 are off	2	110	0	V_{dc}	$-V_{dc}$	$u_2 = 0 + j1.155$
S3,S4,S2 are on S6,S1,S5 are off	3	010	$-V_{dc}$	V_{dc}	0	$u_3 = -1 + j0.577$
S4,S5,S3 are on S1,S2,S6 are off	4	011	$-V_{dc}$	0	V_{dc}	$u_4 = -1 - j0.577$
S5,S6,S4 are on S2,S3,S6 are off	5	001	0	$-V_{dc}$	V_{dc}	$u_5 = 0 - j1.155$
S6,S1,S5 are on S3,S4,S2 are off	6	101	V_{dc}	$-V_{dc}$	0	$u_6 = 1 - j0.577$
S1,S3,S5 are on S4,S6,S2 are off	7	111	0	0	0	$u_7 = 0$
S4,S6,S2 are on S1,S3,S5 are off	8	000	0	0	0	$u_8 = 0$

Table 3.1 Switch States for Three Phase Voltage Source Inverter (VSI)

The non-zero vectors $\bar{u}_1 \ldots \bar{u}_6, d = V_{dc}\sin(60)\bar{u}_0\bar{u}_7$, create a hexagon of Fig.3.1 centered in the origin of the $\alpha - \beta$ plane, with the internal diameter $d = \frac{2}{3}V_{dc}\sin(60)$ and the external diameter $d = \frac{2}{3}V_{dc}$. The zero voltage vectors are located in the origin of the $\alpha - \beta$ plane ($\bar{u}_7$= 111 and $\bar{u}_0$= 000) and they both short circuit the load. Any reference vector u^* located inside the hexagon, Fig. 3.1, can be realized within one switching cycle T_S as a time average of three voltage vectors. The maximum non-distorted output which can be obtained is when the vector u^* tracks the circular locus inscribed into the hexagon. That voltage represents the physical limit obtainable without distortion and is 15.4% higher than the maximum voltage obtained with sinusoidal modulation. Referring to Fig. 3.1, it is impossible to reach all the points on the circle that is circumscribed around the hexagon. Moreover, the modulation can be arranged in such a way that the output voltage u^* tracks the hexagon boundaries, but then the voltage components u_α and u_β will be non-sinusoidal. The best tracking of the reference voltage u^* is obtained when the switching sequence includes only the two vectors adjacent to u^* and a zero vector.

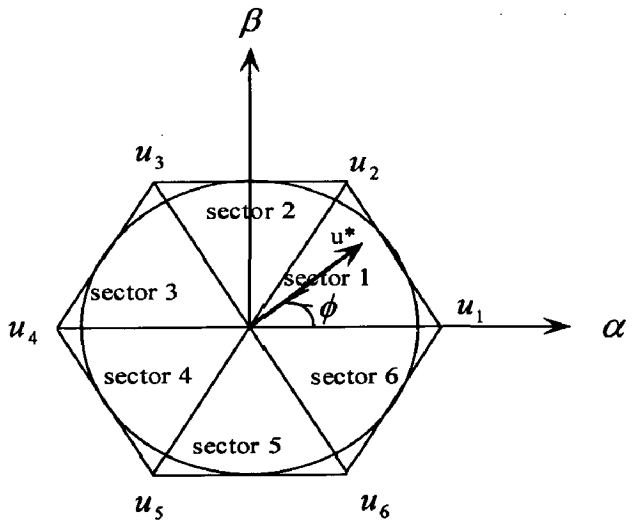

Fig., 3.1 Representation of Rotating Vector in Complex Plane

The time intervals T_1, T_2, and T_0 (Fig 3.2), determine the duration of the three vectors that compose the switching sequence. These intervals depend on the amplitude and the spatial orientation of the reference vector u^*. Assume first that the reference u^* is

in sector 1, Fig.3.1 and that it has an amplitude $|u^*|$ and the angle $\phi = \arg(u^*)$ with respect to the α-axes. The two adjacent non-zero voltage vectors are u_1 and u_2. The intervals T_1, T_2, and T_0 can be determined from the V_d, V_q and angle of the voltage vector position, which can be calculated from V_{an}, V_{bn}, and V_{cn} is shown below.

3.2.2 Three phase to two phase transformation:

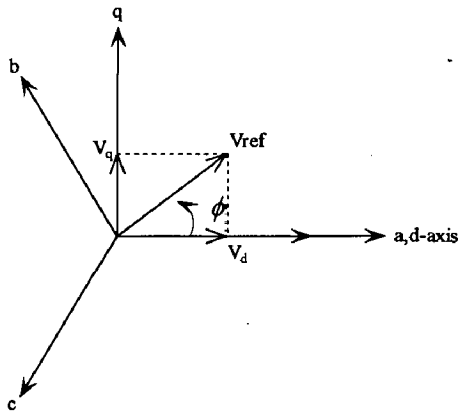

Fig 3.2 Voltage Space Vector and its components in (d,q)

$$V_d = V_{an} - V_{bn}.\cos 60 - V_{cn}.\cos 60 \tag{3.3}$$

$$V_d = V_{an} - \frac{1}{2}V_{bn} - \frac{1}{2}V_{cn} \tag{3.4}$$

$$\begin{aligned} V_q &= 0 + V_{bn}.\cos 30 - V_{cn}.\cos 30 \\ &= 0 + \frac{\sqrt{3}}{2}V_{bn} - \frac{\sqrt{3}}{2}V_{cn} \end{aligned} \tag{3.5}$$

$$\begin{bmatrix} V_d \\ V_q \end{bmatrix} = \frac{2}{3}\begin{bmatrix} 1 & -\frac{1}{2} & -\frac{1}{2} \\ 0 & \frac{\sqrt{3}}{2} & -\frac{\sqrt{3}}{2} \end{bmatrix}\begin{bmatrix} V_{an} \\ V_{bn} \\ V_{cn} \end{bmatrix} \tag{3.6}$$

$$\begin{aligned} |V_{ref}| &= \sqrt{V_d^{\,2} + V_q^{\,2}} \\ \phi &= \tan^{-1}\left(\frac{V_q}{V_d}\right) = \omega_c t = 2\pi f_c t \end{aligned} \tag{3.7}$$

where f_c=fundamental frequency

3.2.3 Estimation of T_1,T_2, and T_0

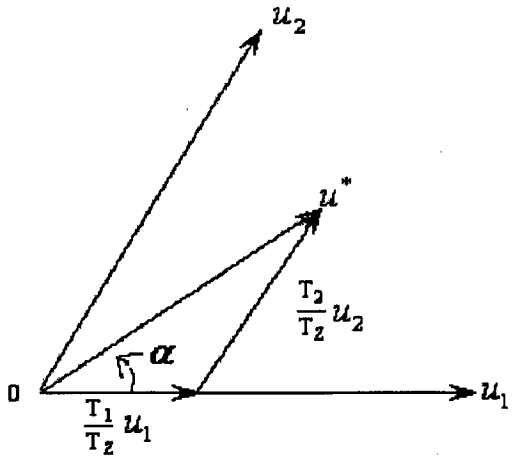

Fig 3.3 Reference vector as a combination of adjacent vectors at sector 1

From the above figure,

$$\int_0^{T_z} u^* dt = \int_0^{T_1} u_1 dt + \int_{T_1}^{T_1+T_2} u_2 dt + \int_{T_1+T_2}^{T_z} u_0 dt \tag{3.8}$$

$$\therefore T_z.u^* = T_1 u_1 + T_2 u_2 \tag{3.9}$$

From the figure

$$T_z\left|V_{ref}\right|\begin{bmatrix}\cos(\alpha)\\ \sin(\alpha)\end{bmatrix} = T_1.\frac{2}{3}.V_{dc}.\begin{bmatrix}1\\0\end{bmatrix} + T_2.\frac{2}{3}.V_{dc}.\begin{bmatrix}\cos(\alpha)\\ \sin(\alpha)\end{bmatrix}$$

$$where, 0 \le \alpha \le 60^o \tag{3.10}$$

$$\therefore T_1 = T_z.M.\frac{\sin\left(\frac{\pi}{3}-\alpha\right)}{\sin\left(\frac{\pi}{3}\right)} \tag{3.11}$$

$$\therefore T_2 = T_z.M.\frac{\sin\ \alpha}{\sin\left(\frac{\pi}{3}\right)} \tag{3.12}$$

$$\therefore T_0 = T_s - T_1 - T_2, \left(where, T_z = \frac{1}{f_s} and M = \frac{\left|V_{ref}\right|}{\frac{2}{3}V_{dc}} \right) \tag{3.13}$$

WhereT_1,T_2,T_0 represent the time widths for vectors $\underline{U}_1$,U_2,U_0.T_0 is the period in a sampling period for null vectors should be filled. As each switching period (half of sampling period) Tz starts and ends with zero vectors i.e. there will be two zero vectors per Tz or four null vectors per Ts, duration of each null vector is To/4. The null time has been conveniently distributed between the U_0 and U_7 vectors to describe the symmetrical pulse width. Studies have shown that a symmetrical pulse pattern gives minimal output harmonics.

3.2.4 Generalized formulas to any Sector

The Switching time duration any sector can be estimated from the following equations [25]

$$T_1 = \frac{\sqrt{3}T_z|V_{ref}|}{V_{dc}}\sin\left(\frac{\pi}{3}-\alpha+\frac{n-1}{3}\pi\right) = \frac{\sqrt{3}T_z|V_{ref}|}{V_{dc}}\sin\left(\frac{n}{3}\pi-\alpha\right) \tag{3.14}$$

$$T_2 = \frac{\sqrt{3}T_z|V_{ref}|}{V_{dc}}\sin\left(\alpha-\frac{n-1}{3}\pi\right) \tag{3.15}$$

$$\therefore T_0 = T_s - T_1 - T_2 \begin{pmatrix} where, n = 1 to 6 \\ 0 \le \alpha \le 60^o \end{pmatrix} \tag{3.16}$$

3.3 Principles of Fuzzy logic

3.3.1 Introduction

Due to continuously developing automation systems and more demanding control performance requirements, conventional control methods are not always adequate. The input output relations of the system may be uncertain and they can be changed by unknown external disturbances. New schemes are needed to solve such problems. One such an approach is to utilize fuzzy control. Fuzzy control is based on fuzzy logic, which provides an efficient method to handle in exact information as basis reasoning. With fuzzy logic it is possible to convert knowledge, which is expressed in an uncertain form,

to an exact algorithm. In fuzzy control, the controller can be represented with linguistic If-then rules, the interpretation of the controller are the fuzzy but controller is processing exact input input-data and is producing exact output-data in a deterministic way.

Fuzzy logic has come a long way since it was first subjected to technical scrutiny in 1965 by Dr. lotfi Zadeh, of the University of California, when he published his seminal work in the journal "information and control". Many theoretical developments in fuzzy logic took place in the US, Europe, and Japan. But the industrial application of the first fuzzy controller was introduced by E.H. Mamdani in 1974. From the mid 1970s Japanese researchers have been a primary force in advancing the practical implementation of the theory. They commercialized this technology and now have 2000 patents all over the world for their products like fuzzy air conditioner, Fuzzy washing machine, cameras and microwave ovens. The applications range from these consumer products to industrial process control, medical instrumentation and decision-support systems. Fuzzy systems have obtained a major role in engineering systems and consumer's products in 1980s and 1990s. New applications are presented continuously.

3.4Structure of a fuzzy controller

Fuzzy control is a control method based on fuzzy logic. Fuzzy logic can be described as "computing with words rather than numbers", and "control with sentences rather than equations". There are specific components characteristic of a fuzzy controller to support a design procedure. In the block diagram in fig3.4 the controller is between preprocessing and post processing blocks

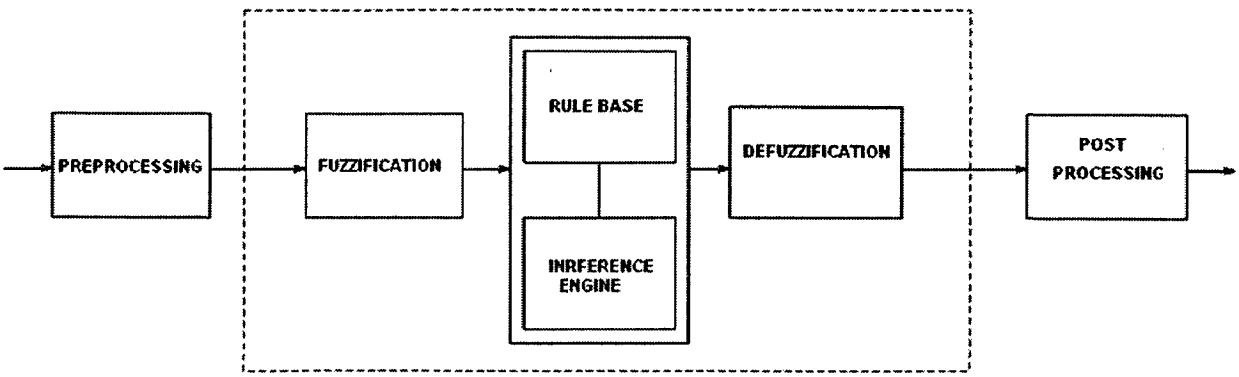

Fig. 3.4 Blocks of a Fuzzy Controller

3.4.1 Preprocessing

The inputs are most often hard or crisp measurements from some measuring equipment, rather than linguistic. Pre processor conditions the measurements before they enter the controller and the control strategy is a static mapping between input and control signal. A dynamic controller would have additional inputs like derivatives, integrals. These are created in preprocessor thus making the controller multidimensional, which requires many rules and makes it more difficult to design. The preprocessor then passes the data on to the controller.

3.4.2 Fuzzification

The first block inside the controller is fuzzification, which converts input data to degrees of membership by lookup in various membership functions. The fuzzification block thus matches the input with the conditions of the rules to Determines how well the condition of each rule matches that particular instance. There is a degree of membership for each linguistic term that applies to that input variable,

3.4.3 Rule base

The rule base is to do with the fuzzy inference rules. It will be usually in an If-then format.

E.g. Inputs – error, change in error.

Rules: IF error is _ AND change in error is _ THEN output is _

3.4.4 Inference Engine

Aggregation:

This operation is use to find the degree of fulfillment or firing strength of the condition of a rule k. if μ_1, μ_2 are the membership functions of rules 1&2, then the aggregation is their combination:

$$\mu_1 \text{ AND } \mu_2$$

Similarly for other rules aggregation is equivalent to fuzzification, when there is only one input to the controller.

Activation

Activation of a rule is the deduction of the conclusion

Accumulation:

All activated conclusions are accumulated

3.4.5 Defuzzification

The resulting fuzzy set must be converted to a number that can be sent to the process as a control signal is called defuzzification. There are several defuzzification methods.

(a) Mean of max
(b) Bisector of area
(c) Center of gravity

3.4.6 Post Processing

Output scaling is also relevant. In case the output is defined on a standard universe this must be scaled to engineering like meters, volts. This block often contains an output gain that can be tuned, and sometimes also an integrator

3.5 Advantages of Fuzzy

The principal advantage of fuzzy control is

1. The fast convergence with adaptive step size of the control variable: This means that the machine flux decrement starts in the beginning with a large step size, which then gradually decreases so that the optimum flux condition is attained quickly.
2. The additional advantage of fuzzy control is that it can accept inaccurate signals Corrupted with noise.

3. The neural network adds the advantage of fast control implementation, either by a dedicated hardware chip or by digital signal processor (DSP)-based software.
4. The fuzzy estimator improves the stator flux estimation accuracy leading to a smooth trajectory and therefore reducing the torque ripples. This estimator is particularly suited in applications needing high torque at low speed and improves the performance of control strategy.

CHAPTER 4

DIRECT TORQUE CONTROL OF INDUCTION MOTOR USING FUZZY SPACE VECTOR MODULATION TECHNIQUE

4.1 DTC of Induction motor using voltage vector reference based SVM

It is well known that the principle of vector control of induction motor drive is to align the flux and torque current along the d-axis and the q-axis of the reference frame, respectively. The torque can be controlled by the associated current component, once the flux is kept constant. The main theme of direct torque control is to regulate the torque and magnitude of the flux directly with out invoking any concept of field orientation. Following this essential concept, Fig., 4.1 shows the block diagram of the new DTC based induction motor drives. In traditional DTC, the torque and stator flux are controlled to follow their references by Bang-Bang method. In the PI regulation method the errors of torque and stator flux are controlled by two PI regulators and the outputs of regulators give the d, q space voltage vector to control motor directly. As the amplitude and angle phase of voltage vectors are decided by the PI regulation, i.e. an average dynamic control without large fluctuation, it leads to good steady performance in low speed range. It is quite straightforward to implement the PI regulators; however the coefficients of PI need to be selected properly.

As shown in the Fig., 4.1, two PI controllers regulate the flux amplitude and torque respectively. Therefore, both the torque and the magnitude of flux are under control, thereby generating the voltage command for inverter control. It can be said that no decoupling mechanism is required since the flux magnitude and torque can be regulated by the PI controllers.

The inverter is controlled by the SVM technique using symmetrical regular sampling. Therefore, the inverter switching frequency is significantly increased, and the associated torque ripple and current harmonics can be dramatically reduced. To increase the inverter switching frequency for the same sampling frequency, the symmetrical Regular Sampled SVM technique with switching patterns as shown Fig., 4.1 is used to

control the new DTC-based drive. The inverter switching frequency is constant and is equal to sampling frequency. SVM modulator requires calculating several equations online for the switching time periods.

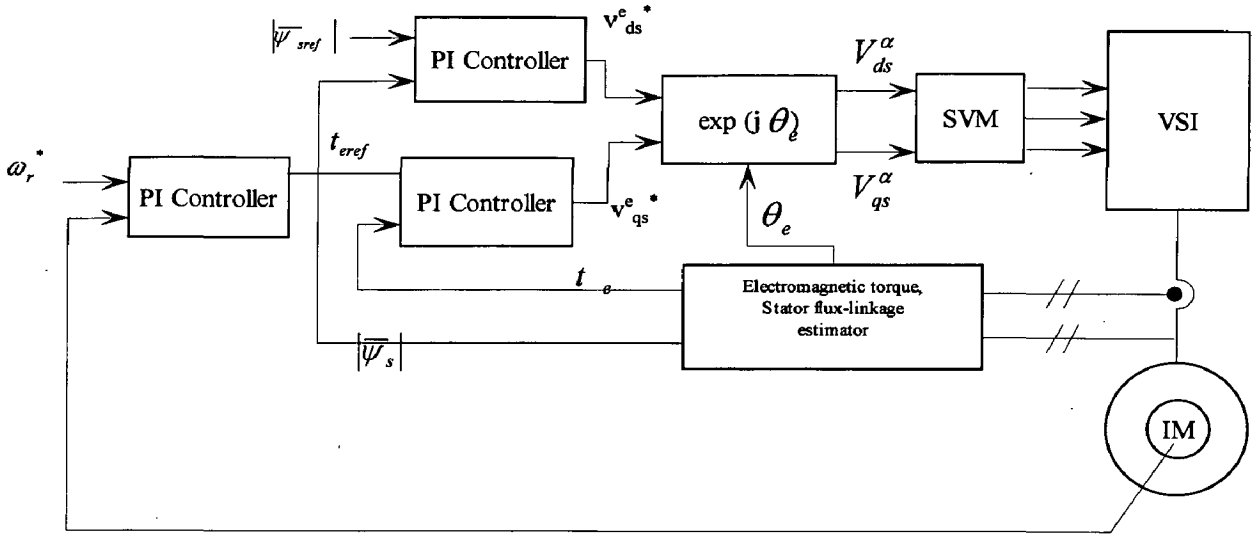

Fig 4.1 The Complete Block diagram of SVM based DTC induction motor drive

The Fig 4.1 shows the complete block diagram of the proposed DTC-based induction motor drive. Where it consists of the Speed controller ,Torque controller, Flux controller which produces Torque reference ,Q-axis voltage reference ,d-axis voltage references respectively and Space Vector Modulator which synthesis the voltages $V_{ds}^{\alpha}{}_{s}$, V_{qs}^{α} to produce required pulses to the inverter.

4.2 Speed Controller, Flux Controller, Torque Controller

The Speed controller, Torque controller, Flux controller are the classical proportional–integral controllers which produces Torque Reference, q-axis voltage reference, d-axis voltage references respectively in rotating reference frame. They can be transformed into stationary reference frame by rotating through the vector block $e^{j\theta_e}$.

4.3 Space Vector Modulation

To implement the space vector pulse width modulator in voltage source inverter, the first task is to find the two switching vectors (from the six non-zero vectors as explained in chapter 3) which are adjacent to the reference voltage space vector (i.e. the

output of the transformation block). From the two adjacent vectors the magnitude of the reference stator voltage space vector is calculated. Then the position of the reference stator voltage space vector is found. The position of the vector and magnitude is checked continuously and the time periods for the switching pulses of the two adjacent switching vectors and Null vector are calculated using the Eqn. (3.2). And the pulses are generated as explained in SV sequence in the chapter 3.

4.4 Voltage Source Inverter

The structure of a typical three phase VSI is shown in Fig. (2.3). As shown below V_a, V_b, V_c are the output voltages of the inverter. S1 through S6 are the six power transistors that shape the output, which are controlled by S1 to S6. When an upper transistor is switched on, the corresponding lower transistor is switched off. The on and off states of the upper transistors, S1, S3, S5 are sufficient to evaluate output voltage.

The relationship between the switching variable vector $[S1, S2, S3]^T$ and the phase output voltage vector $[V_a, V_b, V_c]^T$ is given below .

$$\begin{pmatrix} V_a \\ V_b \\ V_c \end{pmatrix} = \frac{1}{3} V_{dc} \begin{pmatrix} 2 & -1 & -1 \\ -1 & 2 & -1 \\ -1 & -1 & 2 \end{pmatrix} \begin{pmatrix} S1 \\ S2 \\ S3 \end{pmatrix} \qquad (4.1)$$

4.5 Induction Motor

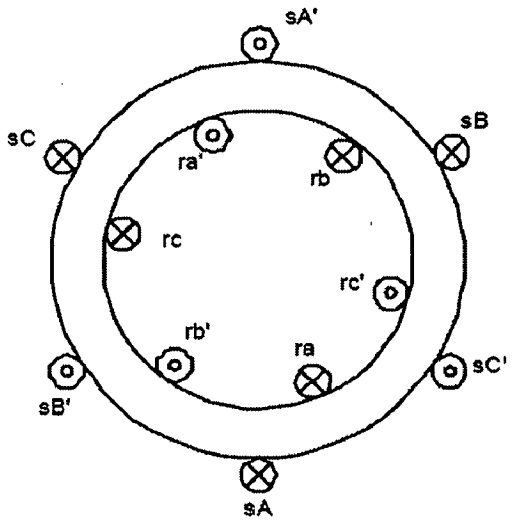

Fig 4.2 a cross view of a three-phase induction motor

Fig 4.2 shows a cross view of a three-phase induction motor ,with the stator and rotor coils represented by concentrated windings .Voltage equations can be written for the stator and rotor phases in terms of self and mutual inductances .As the rotor moves the mutual inductances between the rotor and stator coils change ,because the angle between the axes of the rotor and stator changes .To eliminate the time varying inductances ,the equations are frequently transformed to q-d-0 variables in the arbitrary reference frame .

Fig 3.2 shows a symmetrical 3-phase induction motor with stationary as-bs-cs axes at $2\pi/3$ angle apart which are to be transformed into 2-phase stationary reference frame (d^s-q^s) variables and then to the synchronously rotating reference frame (d^e-q^e) Assume that the d^s-q^s are oriented at θ angle, as shown in Fig. 3.2 .The voltages V_{ds}^s and V_{qs}^s can be resolved into as-bs-cs components and can be represented in the matrix form as

$$\begin{pmatrix} V_{as} \\ V_{bs} \\ V_{cs} \end{pmatrix} = \begin{pmatrix} \cos\theta & \sin\theta & 1 \\ \cos(\theta-120) & \sin(\theta-120) & 1 \\ \cos(\theta+120) & \sin(\theta+120) & 1 \end{pmatrix} \begin{pmatrix} V_{qs}^s \\ V_{ds}^s \\ V_{0s}^s \end{pmatrix} \tag{4.2}$$

The corresponding inverse relation is

$$\begin{pmatrix} V_{qs}^s \\ V_{ds}^s \\ V_{0s}^s \end{pmatrix} = \frac{2}{3} \begin{pmatrix} \cos\theta & \cos(\theta-120) & \cos(\theta+120) \\ \sin\theta & \sin(\theta-120) & \sin(\theta+120) \\ 0.5 & 0.5 & 0.5 \end{pmatrix} \begin{pmatrix} V_{as} \\ V_{bs} \\ V_{cs} \end{pmatrix} \tag{4.3}$$

Where V_{os}^s is added as the zero sequence component, which may or may not be present .We have considered Voltage as the variable. The current and flux linkages can be transformed by similar equations .It is convenient to set $\theta = 0$, so that the q^s-axis is aligned with the as-axis .ignoring the zero sequence component , the transformation relations can be simplified as

$$\begin{aligned} V_{as} &= V_{qs}^s \\ V_{bs} &= -1/2 V_{qs}^s - \sqrt{3}/2 V_{ds}^s \\ V_{cs} &= -1/2 V_{qs}^s + \sqrt{3}/2 V_{ds}^s \end{aligned} \tag{4.4}$$

And inversely

$$V_{qs}^{s} = 2/3V_{as} - 1/3V_{as} - 1/3V_{as}$$
$$V_{ds}^{s} = -1/\sqrt{3}V_{as} + 1/\sqrt{3}V_{as} \qquad (4.5)$$

For this simulation stationary reference frame has been used, which has the advantage of eliminating some terms from the voltage equations. The simulation of the induction motor is accomplished by solving for the flux linkages per second in terms of the voltages applied to the machine .The derivative s of the stator flux linkages are given by Eqn. (4.6) to Eqn. (4.8). In these equations the super script's' indicates the stationary reference frame and the subscript's' indicate the stator quantities.

$$\frac{d}{dt}\Psi_{qs}{}^{s} = V_{qs}{}^{s} + \frac{R_s}{L_{ls}}(\Psi_{mq}{}^{s} - \Psi_{qs}{}^{s}) \qquad \ldots.(4.6)$$

$$\frac{d}{dt}\Psi_{ds}{}^{s} = V_{ds}{}^{s} + \frac{R_s}{L_{ls}}(\Psi_{md}{}^{s} - \Psi_{ds}{}^{s}) \qquad \ldots.(4.7)$$

$$\frac{d}{dt}\Psi_{os}{}^{s} = V_{os}{}^{s} + \frac{R_s}{L_{ls}}\Psi_{os}{}^{s} \qquad \ldots.(4.8)$$

Like wise the derivatives of the rotor flux linkages are given by Eqns. (4.9) to (4.11), where in the subscript 'r' indicates rotor quantities

$$\frac{d}{dt}\Psi_{qr}{}^{s} = \omega_r\Psi_{ds}{}^{s} + \frac{R_r}{L_{lr}}(\Psi_{mq}{}^{s} - \Psi_{qs}{}^{s}) \qquad \ldots..(4.9)$$

$$\frac{d}{dt}\Psi_{dr}{}^{s} = -\omega_r\Psi_{qr}{}^{s} + \frac{R_r}{L_{lr}}(\Psi_{md}{}^{s} - \Psi_{dr}{}^{s}) \qquad \ldots..(4.10)$$

$$\frac{d}{dt}\Psi_{or}{}^{s} = V_{or}{}^{s} - \frac{R_r}{L_{lr}}\Psi_{or}{}^{s} \qquad \ldots..(4.11)$$

The mutual flux linkages denoted by φ_{md}^{s} and φ_{mq}^{s} are given by Eqns. (4.12) to (4.14)

$$\Psi_{mq}{}^{s} = L_{ml}\left(\Psi_{mq}{}^{s}/L_{ls} - \Psi_{qs}{}^{s}/L_{lr}\right) \qquad \ldots..(4.12)$$

$$\Psi_{md}{}^{s} = L_{ml}\left(\Psi_{ds}{}^{s}/L_{ls} - \Psi_{dr}{}^{s}/L_{lr}\right) \qquad \ldots..(4.13)$$

$$L_{ml} = \frac{1}{\frac{1.0}{L_{ml}} + \frac{1.0}{L_{ls}} + \frac{1.0}{L_{lr}}} \qquad \text{.....(4.14)}$$

The stator and rotor currents in the stationary reference frame can then be found by using Eqns. (4.15) to (4.18)

$$i_{qs}^{s} = \frac{1}{L_{ls}}\left(\Psi_{qs}{}^{s} - \Psi_{mq}{}^{s}\right) \qquad \text{.....(4.15)}$$

$$i_{ds}^{s} = \frac{1}{L_{ls}}\left(\Psi_{ds}{}^{s} - \Psi_{md}{}^{s}\right) \qquad \text{.....(4.16)}$$

$$i_{qr}^{s} = \frac{1}{L_{lr}}\left(\Psi_{qr}{}^{s} - \Psi_{mq}{}^{s}\right) \qquad \text{.....(4.17)}$$

$$i_{dr}^{s} = \frac{1}{L_{lr}}\left(\Psi_{dr}{}^{s} - \Psi_{md}{}^{s}\right) \qquad \text{....(4.18)}$$

Substituting Eqns. (4.12) and (4.13) in Eqns. (4.6) and (4.7) we get,

$$\begin{aligned}\frac{d}{dt}\Psi_{qs}{}^{s} &= V_{qs}{}^{s} + \frac{R_s}{L_{ls}}\left(L_{ml}\left(\Psi_{mq}{}^{s}/L_{ls} - \Psi_{qs}{}^{s}/L_{lr}\right) - \Psi_{qs}{}^{s}\right) \\ &= V_{qs}{}^{s} - \frac{R_s}{L_{ls}}\left(\Psi_{qs}{}^{s}\left(1 - \frac{L_{ml}}{L_{ls}}\right) - \Psi_{qr}{}^{s}\left(\frac{L_{ml}}{L_{lr}}\right)\right)\end{aligned} \qquad \text{.....(4.19)}$$

$$\begin{aligned}\frac{d}{dt}\Psi_{ds}{}^{s} &= V_{ds}{}^{s} + \frac{R_s}{L_{ls}}\left(L_{ml}\left(\Psi_{ds}{}^{s}/L_{ls} - \Psi_{dr}{}^{s}/L_{lr}\right) - \Psi_{ds}{}^{s}\right) \\ &= V_{ds}{}^{s} - \frac{R_s}{L_{ls}}\left(\Psi_{ds}{}^{s}\left(1 - \frac{L_{ml}}{L_{ls}}\right) - \Psi_{dr}{}^{s}\left(\frac{L_{ml}}{L_{lr}}\right)\right)\end{aligned} \qquad \text{.....(4.20)}$$

The derivatives of the rotor flux linkages are given by the Eqn. (4.21) and (4.22).

$$\frac{d}{dt}\Psi_{qr}{}^{s} = \omega_r \Psi_{dr}{}^{s} + \frac{R_r}{L_{lr}}\left(\Psi_{mq}{}^{s} - \Psi_{qr}{}^{s}\right) \qquad \text{.....(4.21)}$$

$$\frac{d}{dt}\Psi_{dr}{}^{s} = -\omega_r \Psi_{qr}{}^{s} + \frac{R_r}{L_{lr}}\left(\Psi_{md}{}^{s} - \Psi_{dr}{}^{s}\right) \qquad \text{.....(4.22)}$$

Thus, substituting Eqns. (4.12) and (4.13) in the above equations;

$$\frac{d}{dt}\Psi_{qr}{}^{s} = \omega_r \Psi_{dr}{}^{s} - \frac{R_r}{L_{lr}}\left(\Psi_{qr}{}^{s}\left(1+\frac{L_{ml}}{L_{lr}}\right) - \Psi_{qs}{}^{s}\left(\frac{L_{ml}}{L_{ls}}\right)\right) \qquad \text{.....(4.23)}$$

$$\frac{d}{dt}\Psi_{dr}{}^{s} = -\omega_r \Psi_{qr}{}^{s} - \frac{R_r}{L_{lr}}\left(\Psi_{dr}{}^{s}\left(1+\frac{L_{ml}}{L_{lr}}\right) - \Psi_{ds}{}^{s}\left(\frac{L_{ml}}{L_{ls}}\right)\right) \qquad \text{.....(4.24)}$$

Eqns. (4.6) to (4.25) provide electrical quantities. The induction motor is, of course, an electromechanical device so the model also requires expressions for the electromagnetic torque and the speed of the machine.

Eqn. (4.25) expresses the electromagnetic torque in terms of the flux linkages, and Eqn.(4.26)determines the rotational speed from the machine torque ,load torque and moment of inertia .In both of the following equations , P is the number of poles .In this model, the core model neglects core loss as well as friction and windage losses are neglected.

$$T_e = \frac{3}{2}\frac{P}{2}\frac{\left(\Psi_{ds}{}^{s} i_{qs}{}^{s} - \Psi_{qs}{}^{s} i_{ds}{}^{s}\right)}{\omega_b} \qquad \text{.....(4.25)}$$

$$p\omega_r = \frac{P}{2J}\left(T_e - T_{load}\right) \qquad \text{.....(4.26)}$$

The above derived equations are used to construct the Simulink model of Induction Motor.

4.6 Flux and Torque Estimator

The flux and Torque can be estimated from the following equations. [7]

$$\lambda_s^{\alpha} = \int\left(v_s^{\alpha} - R_s i_s^{\alpha}\right)dt \qquad \text{.....(4.27)}$$

$$T_e = 3\frac{P}{2}\left(\lambda_d^{\alpha} i_q^{\alpha} - \lambda_q^{\alpha} i_d^{\alpha}\right) \qquad \text{....(4.28)}$$

Where λ_{ds}^{α} , λ_{qs}^{α} are the stator d-axis and q-axis flux linkages in stator reference frame . V_{ds}^{α} , V_{qs}^{α} are the stator d-axis and q-axis voltages , i_{ds}^{α} , i_{qs}^{α} are the d-axis and q-axis stator currents in stationary reference frame.

4.7 Modeling of DTC using Voltage vector based SVM

4.7.1 Axis Transformation ($e^{j\theta}$)

The reference voltages n rotating reference frame which are obtained from the Flux and Torque Controller are transformed into stationary reference frame in this block using the following equations.

$$V_{qs}^{\ s} = V_{qs}\cos\theta_e + V_{ds}\sin\theta_e \qquad (4.29)$$

$$V_{ds}^{\ s} = -V_{qs}\sin\theta_e + V_{ds}\cos\theta_e \qquad (4.30)$$

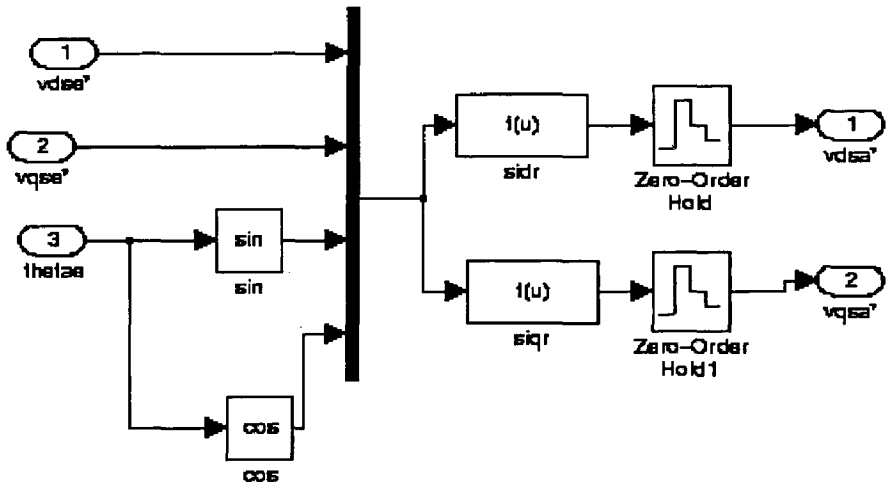

Fig 4.3 Simulink block of the axis transformation

4.7.2 Space Vector Modulation

The reference voltages from the block $e^{j\theta_e}$ are the inputs to this block. From which the angle between the vectors is found and hence the sector is determined, as explained in chapter 3. Then the time for which the active vectors are applied is found by the following equations.

$$T_1 = T_s M \cos(\pi/6+\theta) = T_s M \sin(\pi/3-\theta) \quad (4.41)$$

$$T_2 = T_s M \sin\theta \quad (4.42)$$

$$T_0 = T_s - T_1 - T_2 \quad (4.43)$$

From these switching time periods the standard switching pattern is selected according to the sector and the switching pattern is generated, which is then applied to the Voltage Source Inverter.

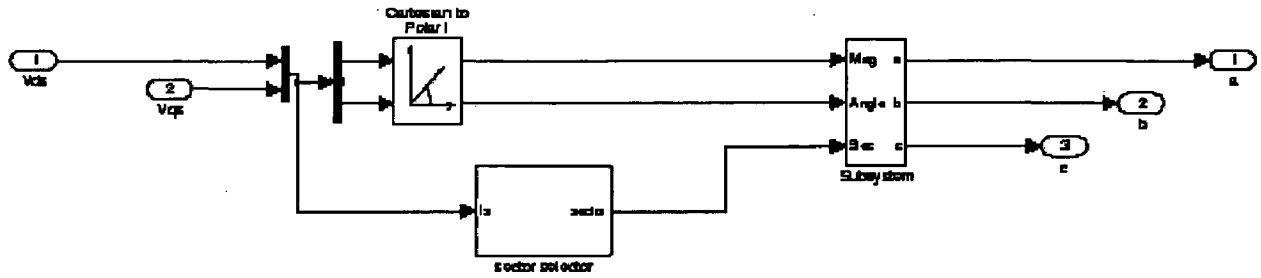

Fig 4.4 Simulink block of the SVM and V.S.I

4.7.3 Voltage Source Inverter

The switching Pulses applied to the Voltage Source Inverter are converted into the phase voltages which are applied to the induction motor are given by the following Matrix.

$$\begin{pmatrix} V_a \\ V_b \\ V_c \end{pmatrix} = \frac{1}{3} V_{dc} \begin{pmatrix} 2 & -1 & -1 \\ -1 & 2 & -1 \\ -1 & -1 & 2 \end{pmatrix} \begin{pmatrix} S1 \\ S2 \\ S3 \end{pmatrix} \quad (4.44)$$

Where S1, S2, S3 are the switching pulses and V_a, V_b, V_c are the phase voltages which are applied to the induction motor.

4.7.4 Induction Machine Model

The Fig. 4.5 shows the flux model simulation of the induction motor which is discussed in 4.5 .The model receives the input voltages V_{ds}^s and V_{qs}^s

Siqs, sids, siqr, sidr are implemented using the Eqns.(4.20), (4.23)and (4.24)respectively.

The d-axis and q-axis Mutual flux linkages are given by the following equations.

$$\Psi_{mq}{}^{s} = L_{ml}\left(\Psi_{mq}{}^{s}/L_{ls} - \Psi_{qs}{}^{s}/L_{lr}\right) \tag{4.45}$$

$$\Psi_{md}{}^{s} = L_{ml}\left(\Psi_{ds}{}^{s}/L_{ls} - \Psi_{dr}{}^{s}/L_{lr}\right) \tag{4.46}$$

Using the above equations the subsystem blocks simd, simq are implemented.

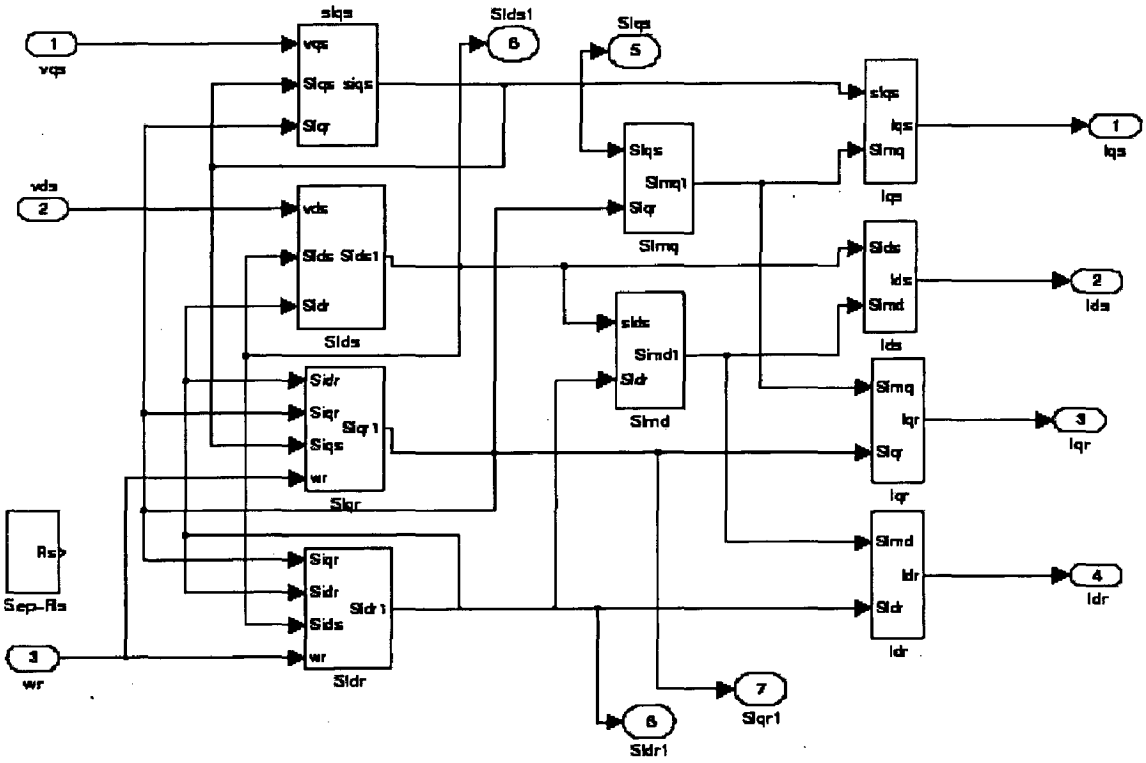

Fig 4.5 Simulink Model of an Induction Machine

Finally the subsystem blocks i_{ds}, i_{qs}, i_{dr}, i_{qr} are implemented using the equations given below.

$$i_{qs}^{s} = \frac{1}{L_{ls}}\left(\Psi_{qs}{}^{s} - \Psi_{mq}{}^{s}\right) \tag{4.47}$$

$$i_{ds}^{s} = \frac{1}{L_{ls}}\left(\Psi_{ds}{}^{s} - \Psi_{md}{}^{s}\right) \tag{4.48}$$

$$i_{qr}^{s} = \frac{1}{L_{lr}}\left(\Psi_{qr}{}^{s} - \Psi_{mq}{}^{s}\right) \tag{4.49}$$

$$i_{dr}^{s} = \frac{1}{L_{lr}}\left(\Psi_{dr}{}^{s} - \Psi_{md}{}^{s}\right) \tag{4.50}$$

Thus the Torque and Speed are estimated using the following equations.

$$T_e = \frac{3}{2}\frac{P}{2}\frac{\left(\Psi_{ds}{}^{s} i_{qs}{}^{s} - \Psi_{qs}{}^{s} i_{ds}{}^{s}\right)}{\omega_b} \tag{4.51}$$

$$p\omega_r = \frac{P}{2J}\left(T_e - T_{load}\right) \tag{4.52}$$

4.7.5 Flux and Torque Estimation

The flux and Torque is estimated by using the following equations[7]

$$\lambda_{ds}^{\alpha} = \int\left(v_{ds}^{\alpha} - R_s i_{ds}^{\alpha}\right)dt \tag{4.53}$$

$$\lambda_{qs}^{\alpha} = \int\left(v_{qs}^{\alpha} - R_s i_{qs}^{\alpha}\right)dt \tag{4.54}$$

$$T_e = 3\frac{P}{2}\left(\lambda_d^{\alpha} i_q^{\alpha} - \lambda_q^{\alpha} i_d^{\alpha}\right) \tag{4.55}$$

Where $\lambda_{ds}^{\alpha}, \lambda_{qs}^{\alpha}$ are the stator d-axis and q-axis flux linkages in stator reference frame. $V_{ds}^{\alpha}, V_{qs}^{\alpha}$ are the stator d-axis and q-axis voltages $i_{ds}^{\alpha}, i_{qs}^{\alpha}$ are the d-axis and q-axis stator currents in stationary reference frame .

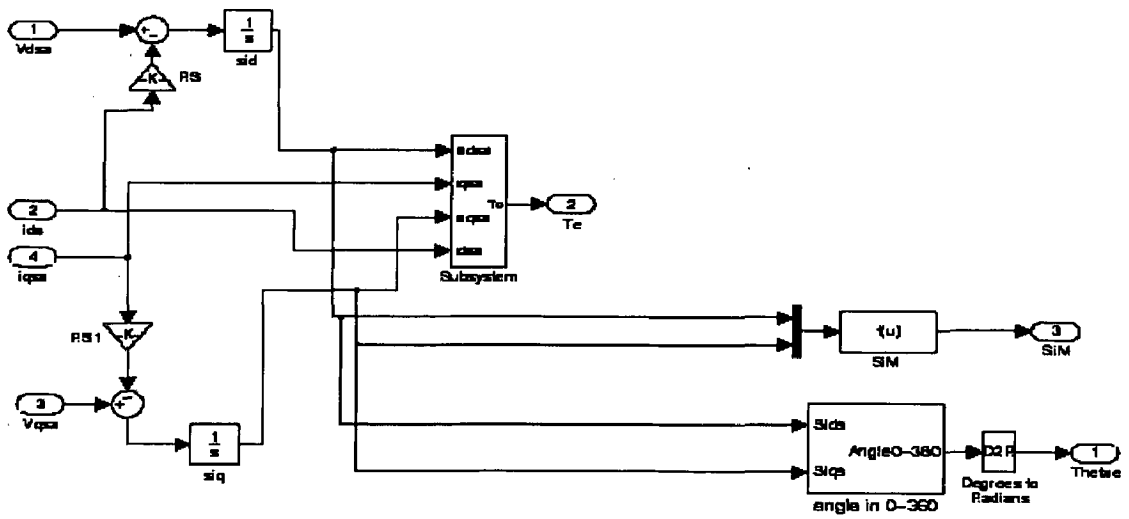

Fig 4.6 Simulink block of the Flux and Torque Estimator

4.8 Direct Torque Control of Induction motor Drive using fuzzy logic based Space Vector Modulation

4.8.1 General

In the former method the control is achieved by generating voltage reference u_s^* based upon the errors of torque and flux and the position of the stator flux position. In that method the d-q components of the reference voltage vector u_s^* is generated by the two PI controllers by processing the errors of the torque and flux. In the present method direct torque control of induction motor drive is achieved using fuzzy logic based space vector modulation. Using fuzzy logic technique, the reference space voltage vector can be obtained dynamically in terms of torque error, stator flux error and the angle of stator flux. Flux and torque errors has been used for obtaining switching states as in feedback PWM [18] and sampled error of the flux is used to generate switching states unlike feedback PWM. In feedback PWM, instantaneous error has been adopted for generation of switching pulses. Where two simple PI controllers are required as compared to three in the voltage vector reference based SVM control method.

Description of the control scheme

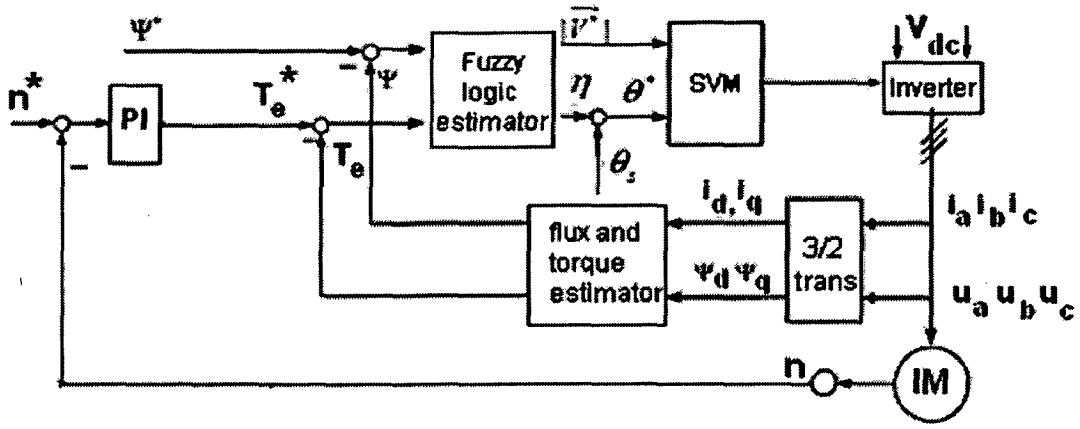

Fig 4.7 The complete block diagram of DTC of induction motor using fuzzy based SVM

As described previously, DTC is direct control of flux and torque within the limits of flux and torque hysteresis bands by selection of optimum inverter switching vectors. Predictive control method in DTC means the deflection angle of required voltage vectors is dynamically regulated, so that, more precise voltage vectors can be applied to the

machine to reduce the ripples of torque and flux. Since the angle η is function of torque error and flux error, a novel fuzzy logic DTC using SVM of IM is presented and shown in Fig 4.8. According to fuzzy logic technique, when angle η is estimated, required voltage space vector is obtained, and SVM is able to adapt to control the machine, instead of using hysteresis comparators and optimum voltage switching vector lookup table as in conventional DTC.

If v* is dynamically obtained on the control of IM, that is its amplitude and space position are adjustable, the ripples of torque and flux are expected to be decreased. As shown in Fig 4.8, in stationary reference frame, the stator flux variation can be resolved in two perpendicular components $\Delta\psi_{sf}$ and $\Delta\psi_{st}$, where $\Delta\psi_{sf}$ affects the stator flux magnitude, and $\Delta\psi_{st}$ influences on torque magnitude. Synthesized space voltage vector V* is in the direction of s, and affects on both and $\Delta\psi_{st}$. Angle of θ* is the controlled variable. Since space position of stator flux can be calculated, the space angle of V* is able to be determined by predicting the angle of V* and stator flux,

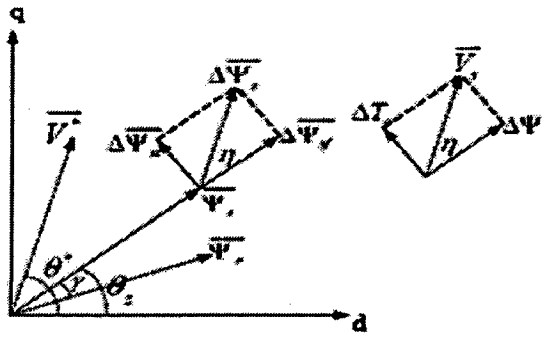

Fig 4.8: space voltage vector and stator flux vector in stationary Reference frame

In the fuzzy logic estimator, there are two input variables, which are absolute torque error $|E_T|$, stator flux error $|E_\Psi|$ one output variable is the deflection angle η of synthesized voltage vector. Each universe of discourse of the torque error, flux error, and deflection angle is divided into four fuzzy sets. Triangle membership functions have been used. All the membership functions (MF) are shown in Fig 4.9 respectively

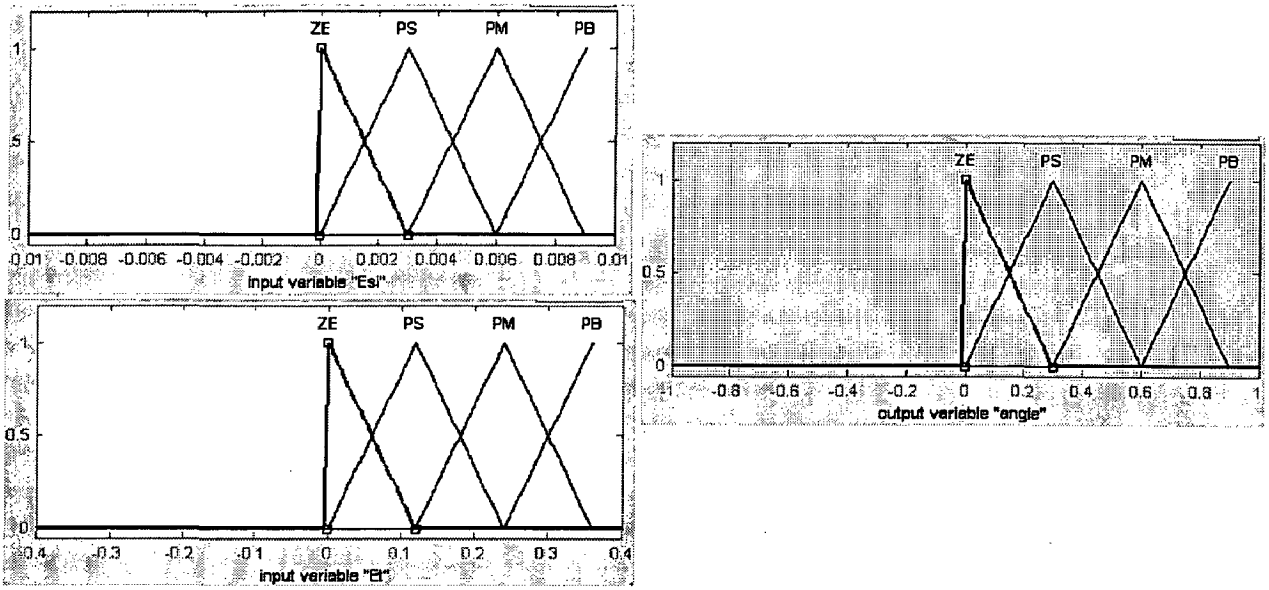

Fig 4.9.membership functions of flux error e_ψ,torque error e_t and angle η

There are total of 16 rules as listed in table 1. Each control rule can be described using the input variables $|E_T|$,$|E_\Psi|$ and control variable η. The i_{th} rule R_i can be expressed as:

R_i : If $|E_T|$ is A_i ,$|E_\Psi|$ is B_i then η is V_i

Where A_i , B_i and V_i denote the fuzzy subsets.

$\lvert E_T\rvert$ \ $\lvert E_\psi\rvert$	ZE	PS	PM	PB
ZE	PS	ZE	ZE	ZE
PS	PM	PS	ZE	ZE
PM	PB	PM	PS	ZE
PB	PB	PB	PM	ZE

Table 4.1 Fuzzy Rule Base For 16 Rules

The inference method used is Mamdani's procedure (inference) based on min-max decision. The firing strength (applied fuzzy operators), for i_{th} rules is given by

$$\alpha_i = \min(\mu_{A_i}(|E_T|), \mu_{B_i}(|E_\psi|)) \qquad \ldots\ldots(4.56)$$

By fuzzy reasoning, Mamdani's minimum procedure (fuzzy inference) gives

$$\mu'_{V_i}(\eta)=\min(\alpha_i,\mu_{V_i}(\eta)) \qquad \text{.....(4.57)}$$

Where μ_A, μ_B and μ_V are membership functions of sets A, B and V of the variables $|E_T|$, $|E_\Psi|$ and η respectively. Thus, the membership function μ_V of the output η is given by

$$\mu_V(\eta)=\max_{i=1}^{16}(\mu'_{V_i}(\eta)) \qquad \text{.....(4.58)}$$

The Maximum criterion method is used for defuzzification, and the final single-valued output is obtained by this method. As stated above, in the case that both torque error and flux error are positive, the angle η is obtained by the fuzzy logic estimator. In the other three cases, deflect angle can be derived simply as follows:

$$\begin{aligned}
&\text{If } |E_T|\geq 0 \text{ and } |E_\psi|\leq 0, \quad \text{then } \eta=\pi-\eta;\\
&\text{If } |E_T|<0 \text{ and } |E_\psi|<0, \quad \text{then } \eta=\pi+\eta;\\
&\text{If } |E_T|<0 \text{ and } |E_\psi|\geq 0, \quad \text{then } \eta=2\pi-\eta
\end{aligned} \qquad \text{.....(4.59)}$$

Finally, the space angle of required space voltage vector is able to be calculated by formula:

$$\theta^*=\theta_s+\eta \qquad \text{.....(4.60)}$$

4.8.3 Speed Controller and Torque Controller

The speed controller and torque controller are classical Proportional-Integrator which produces Torque reference and angle δ respectively.

4.8.4 Modeling of DTC using fuzzy based SVM

Some common blocks have been presented in previous sections.

A. Complete model of Direct Torque Control of Induction motor using Fuzzy Based Space Vector Modulation

The Fig 4.10 shows the complete model for the Direct Torque Control of Induction motor using Fuzzy Based Space Vector Modulation

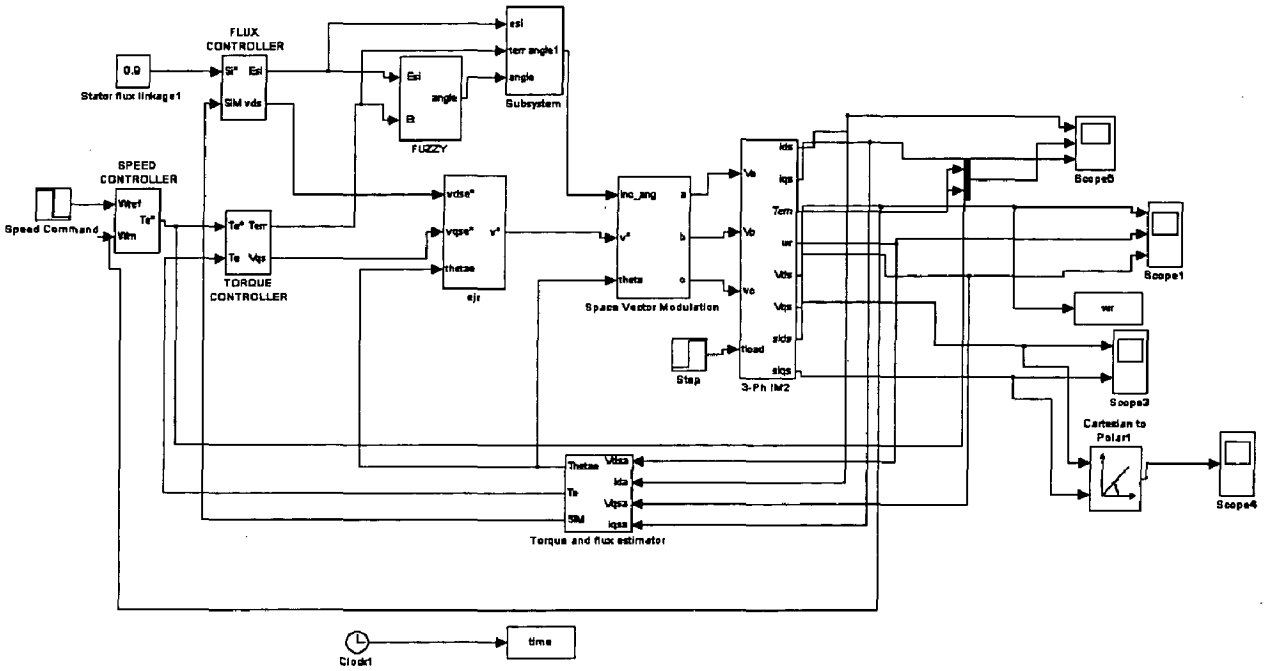

Fig: 4.10 Simulink model of Direct Torque Control of Induction motor using Fuzzy Based Space Vector Modulation

Chapter-5

SIMULATION RESULTS

5.1 Simulation Results for classical DTC of Induction Motor

In order to show the effectiveness of the control scheme a simulation has been carried out on Induction Motor with the specifications given in Appendix. The control scheme is simulated with Matlab/Simulink, which is the most popular and powerful tool for simulation. Fig 5.1 shows phase voltages 'Va, Vb, Vc' of the inverter.

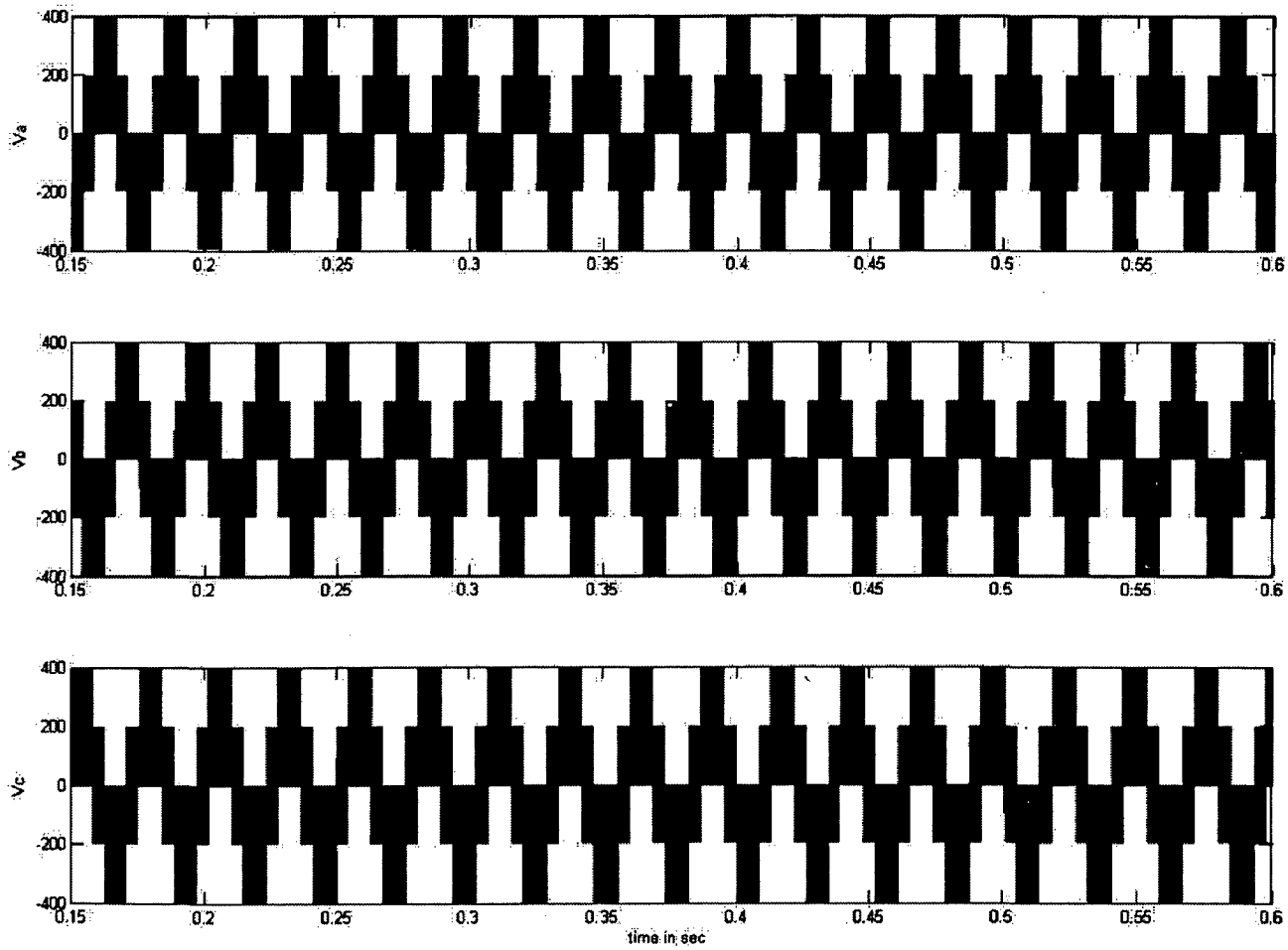

Fig 5.1 phase voltages Va Vb, Vc (volts) Vs time(sec)

Figure 5.2 shows line current of the Induction Motor.

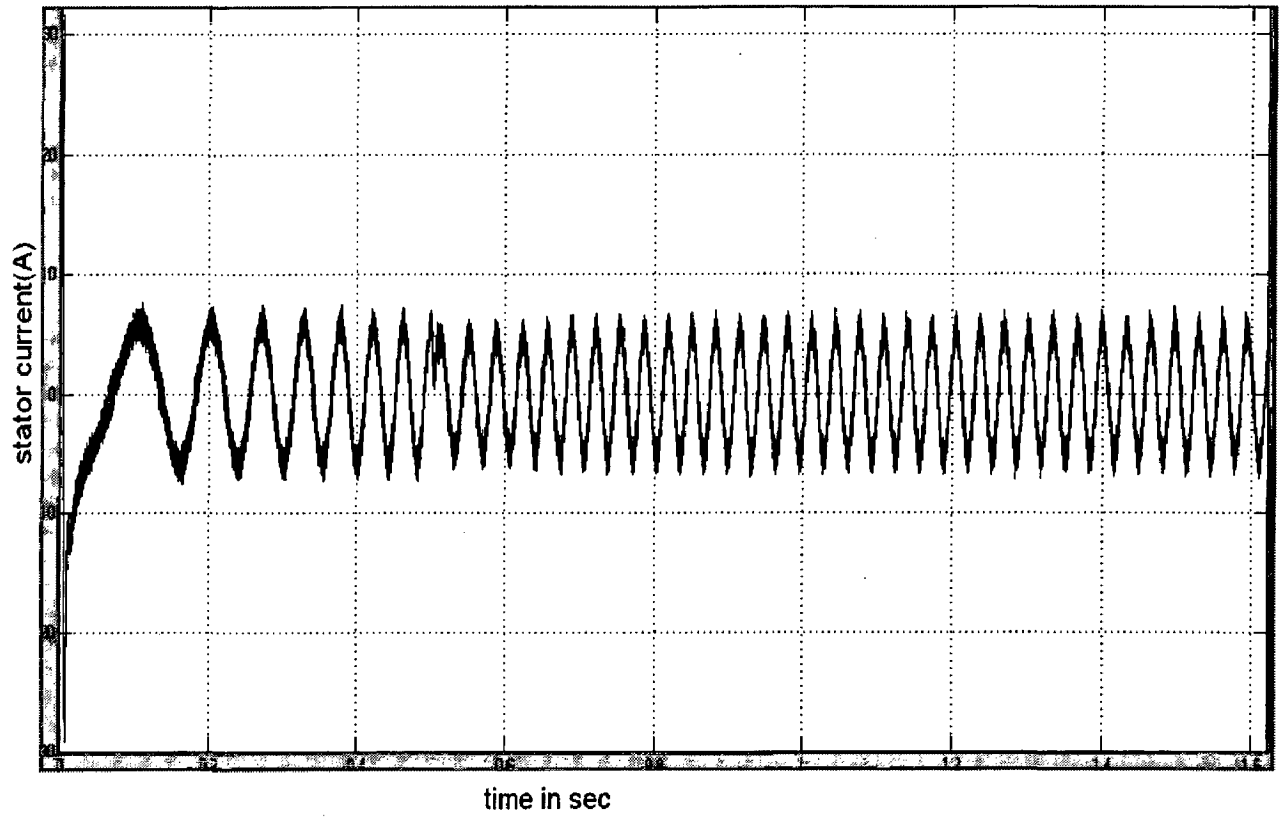

Fig 5.2 line current of the induction motor for classical DTC

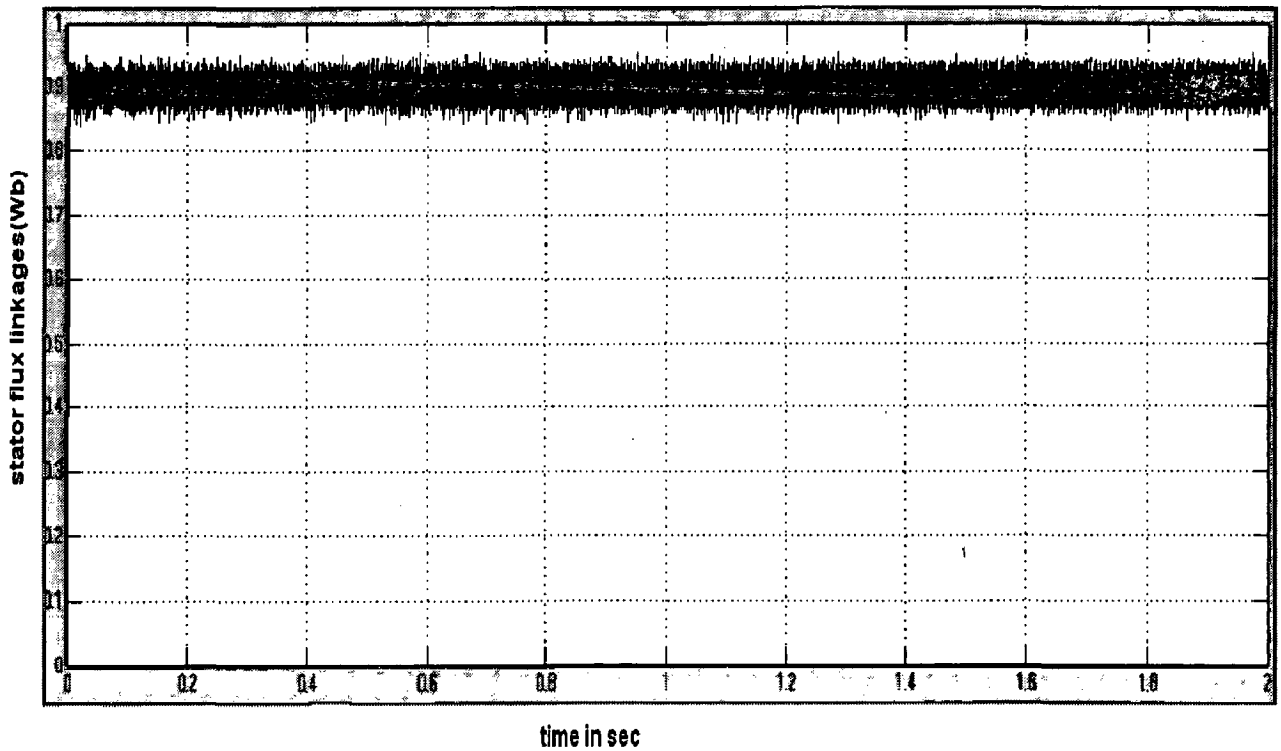

Fig 5.3 Stator flux linkage with respect to time for classical DTC

Fig 5.4 shows the speed, torque response of Induction motor at constant speed command of 1440rpm.

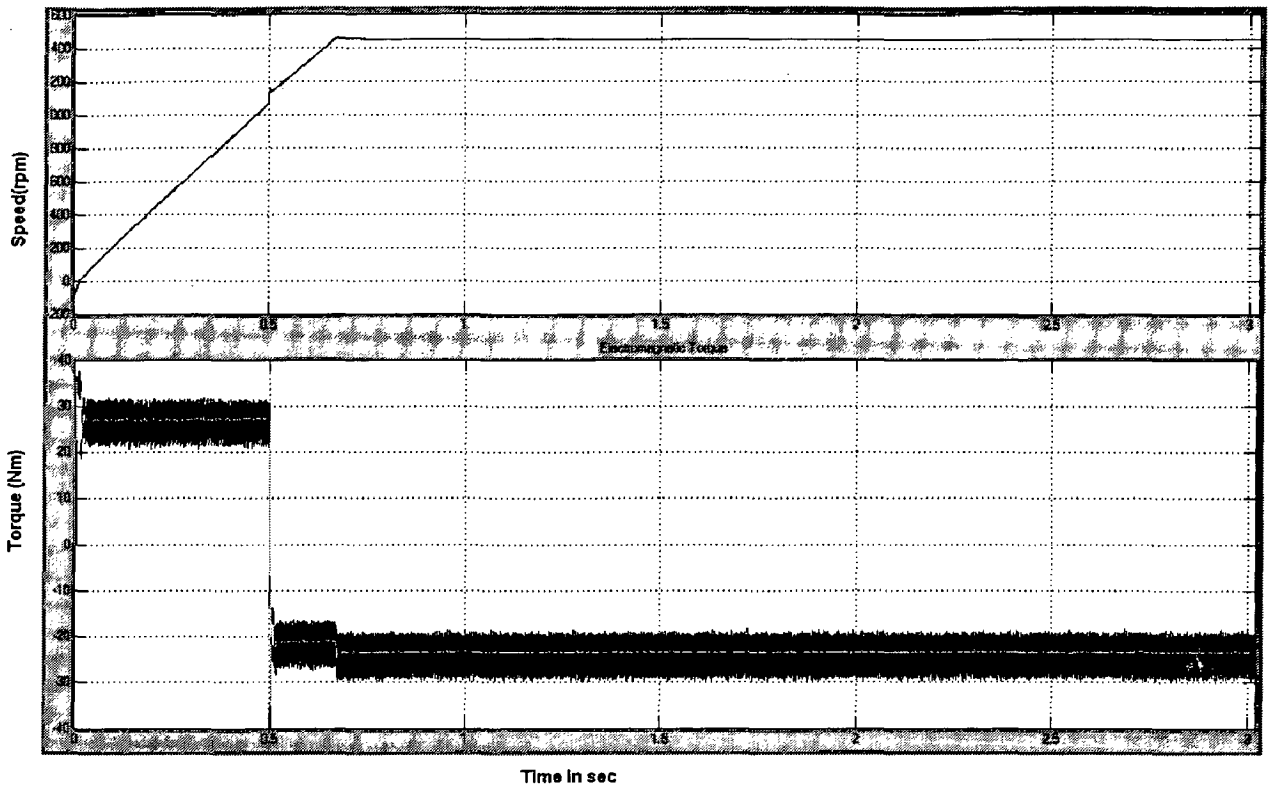

Fig 5.4 Speed and torque response of the induction motor at rated speed and rated torque for classical DTC

5.2 Simulation Results of DTC of Induction Motor using Fuzzy based SVM Technique

Phase voltages 'Va, Vb, Vc' of the inverter

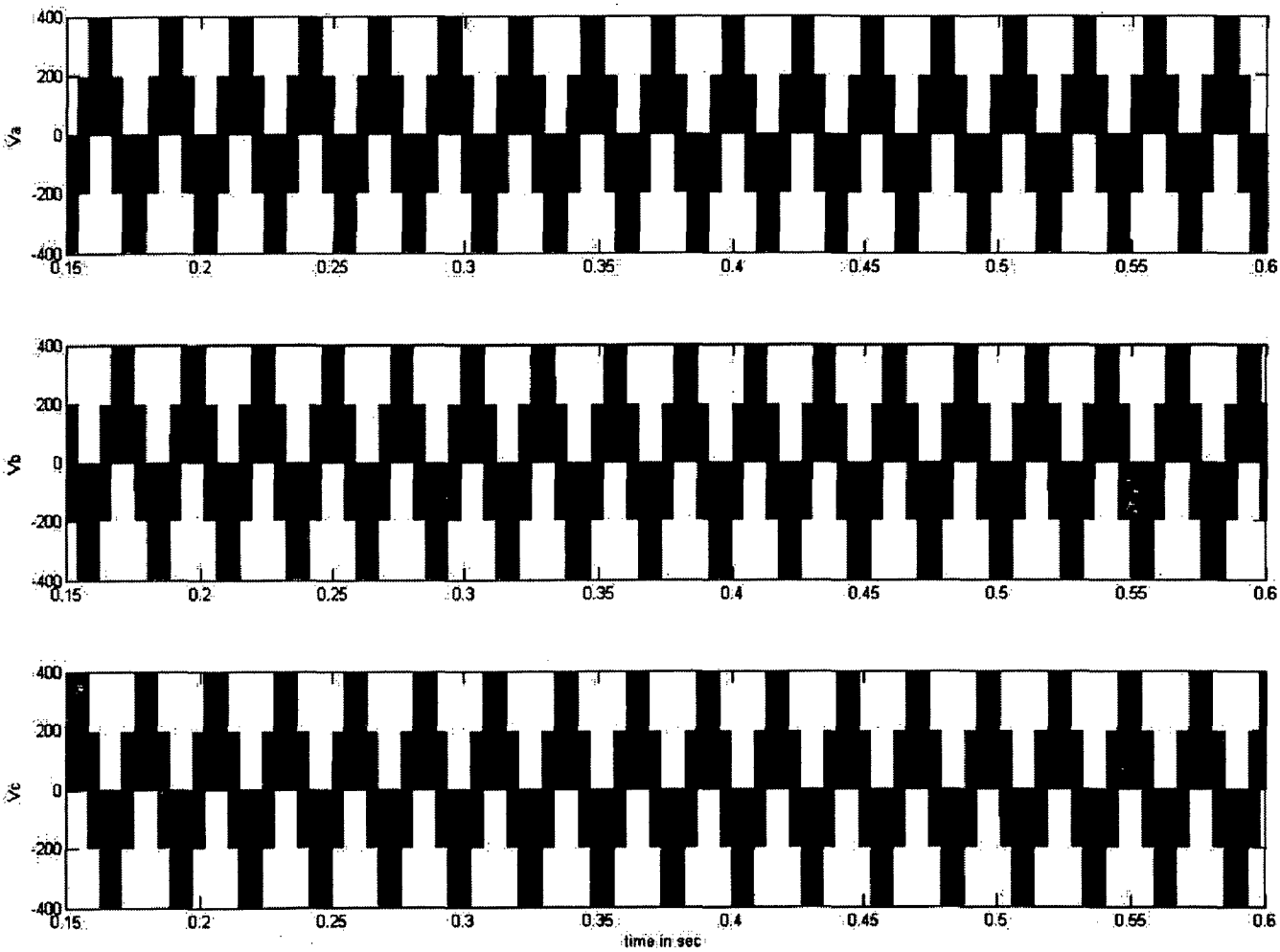

Fig 5.5 phase voltages Va Vb, Vc (volts) Vs time(sec)

Fig 5.6 shows line currents of the Induction Motor.

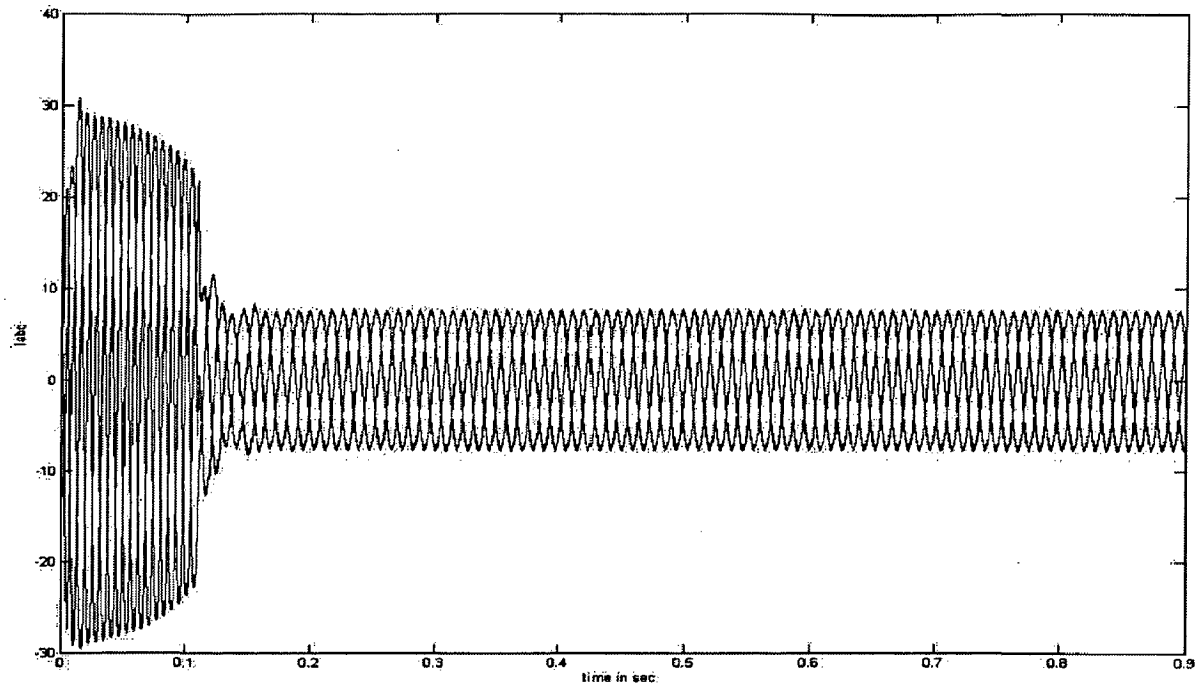

Fig 5.6 Three phase currents of the induction motor with fuzzy svm

Fig 5.7 shows the stator current d-q components of the induction motor

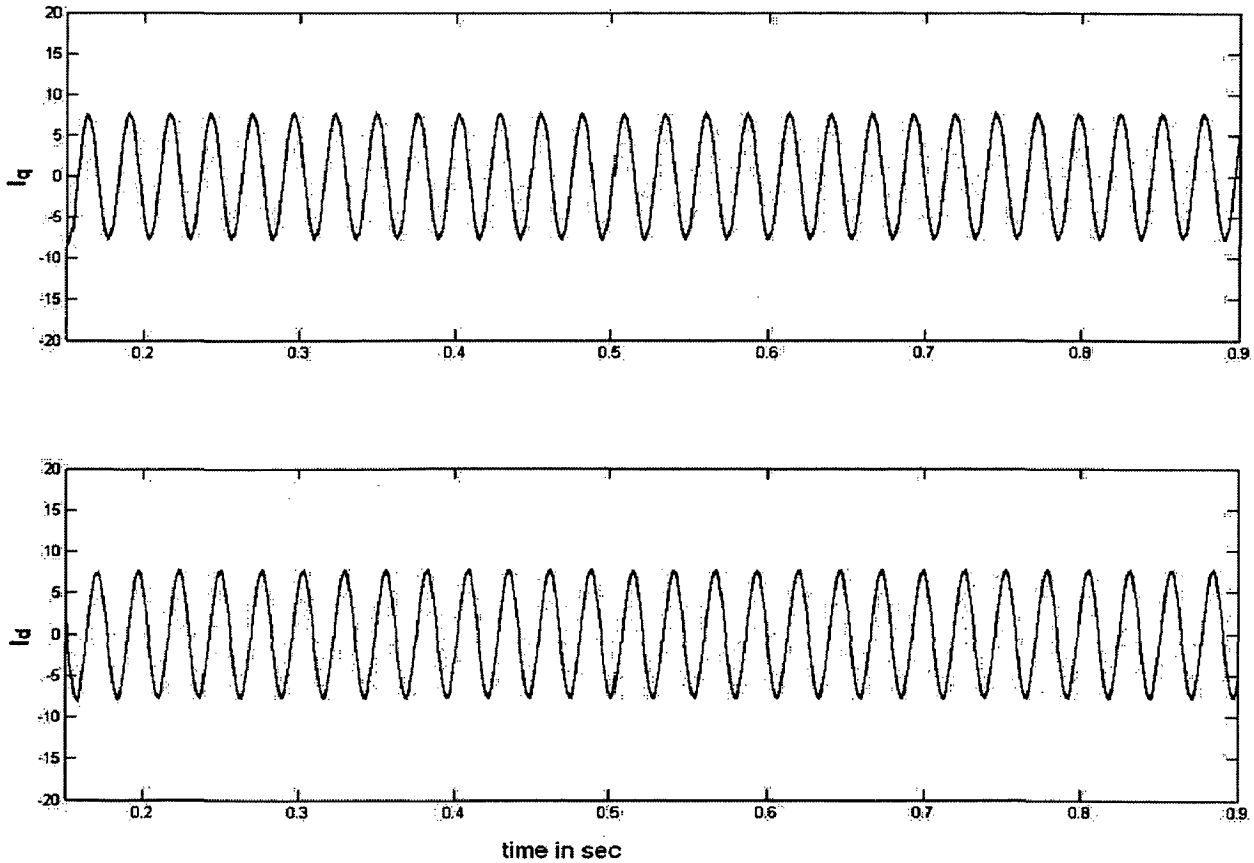

Fig 5.7 d-q components of Stator current Vs time

Fig 5.8 shows the speed, torque response of Induction motor at constant speed command of 1440rpm is applied up to 1 second after1 second -1440 rpm applied and rated load torque 24 N-m applied.

From that figure we can say the system maintains constant speed and at different load torque. Even though the load torque changes continuously the speed is maintained at constant speed.

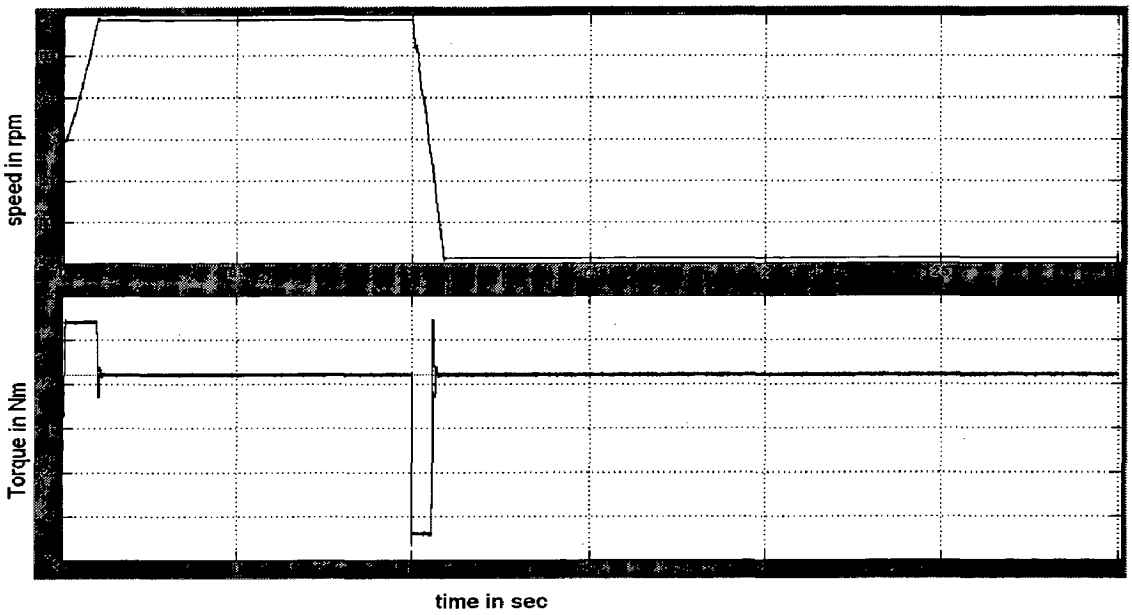

Fig 5.8 Speed and torque response of the induction motor at rated speed and rated torque

Fig 5.9 shows the stator flux linkage with respect to time.

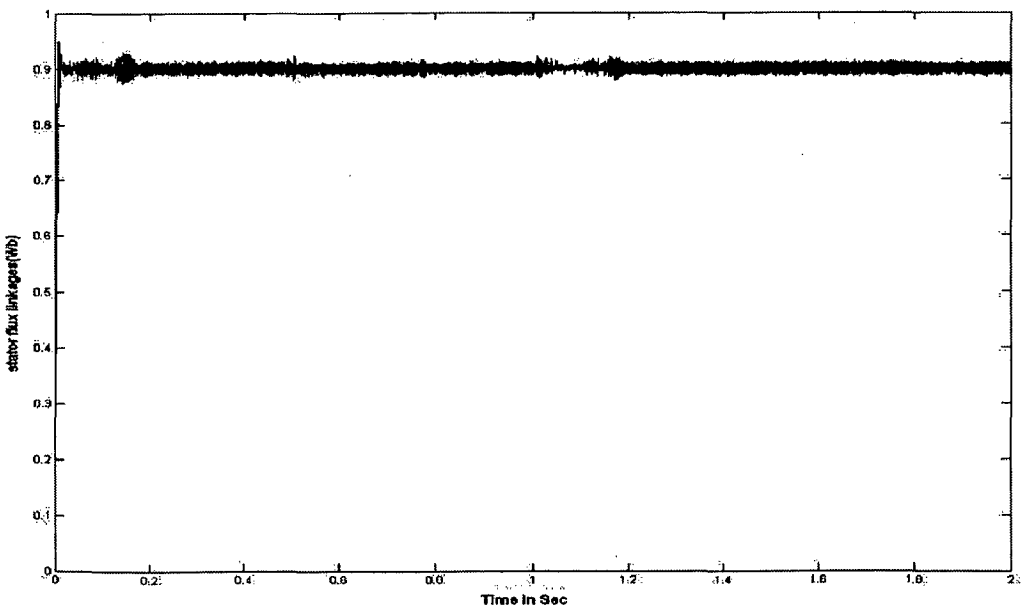

Fig 5.9 Stator flux linkage with respect to time in fuzzy DTC

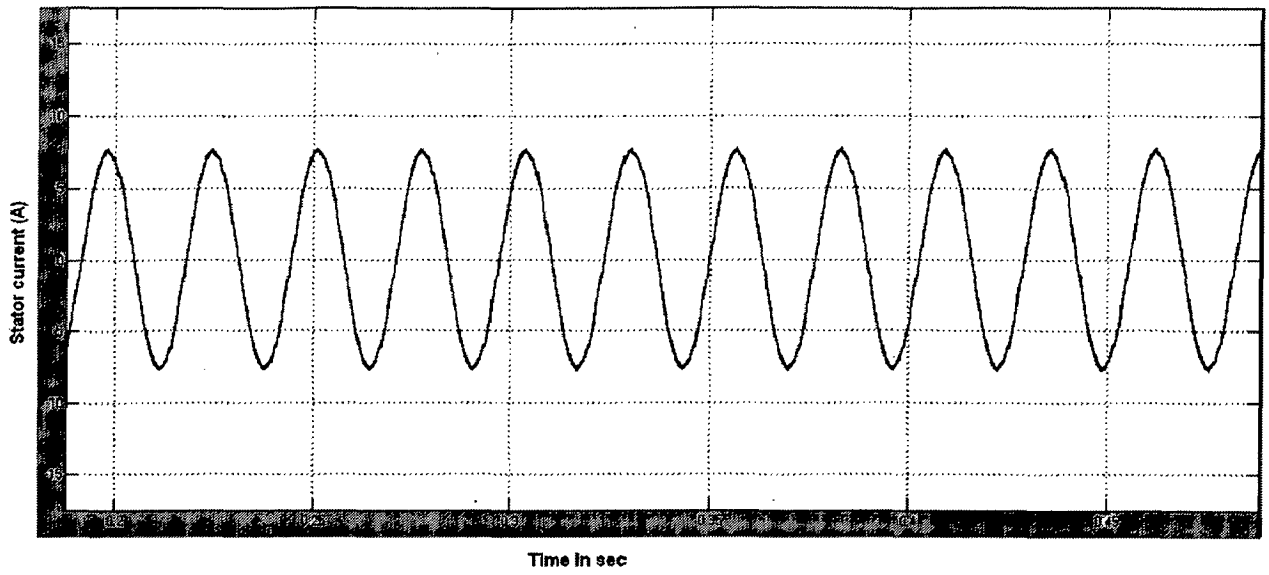

Fig 5.10 stator current for fuzzy DTC

5.2 Comparisons with classical DTC of Induction motor

With the same conditions of speed and torque changes as applied to the previous method the various wave forms are shown below.

Fig 5.11(a) shows the stator flux with respect to time for classical DTC. Figure 5.11(b) shows of the stator flux linkage for the DTC using fuzzy based SVM. From the comparison Fig5.11 (a) and (b), it can be observed that fuzzy based SVM has less flux ripples

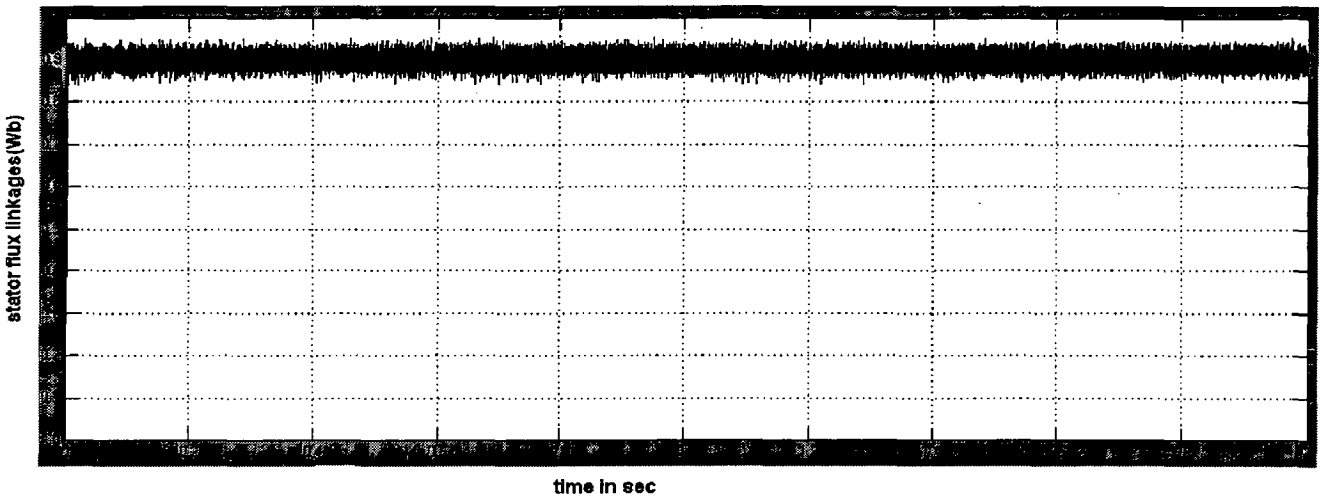

Fig 5.11.(a). Stator flux linkage with respect to time in classical DTC

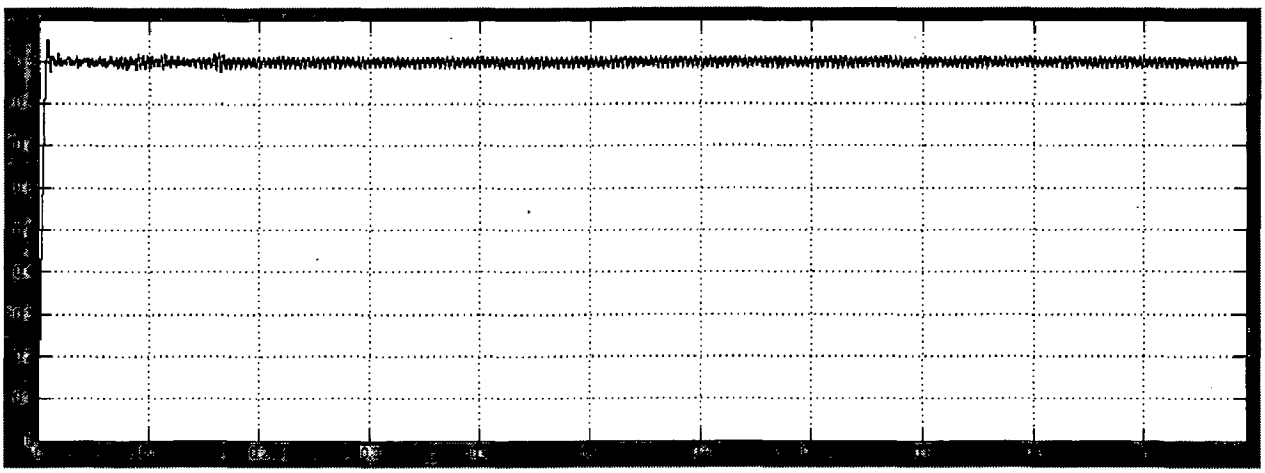

Fig 5.11.(b). Stator flux linkage with respect to time with fuzzy DTC

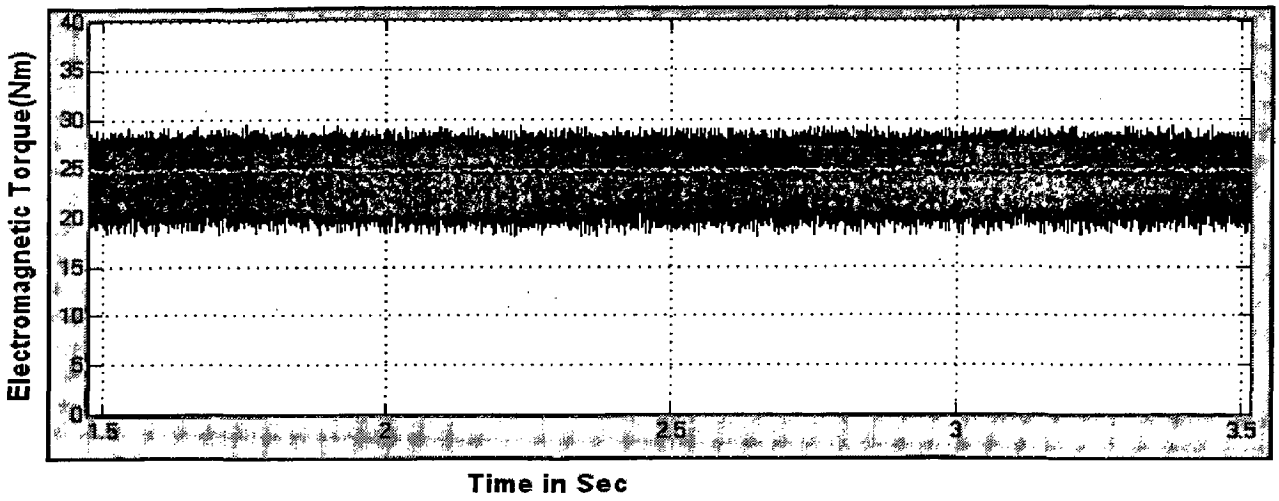

5.12(a) Electromagnetic torque with respect to time in classical DTC

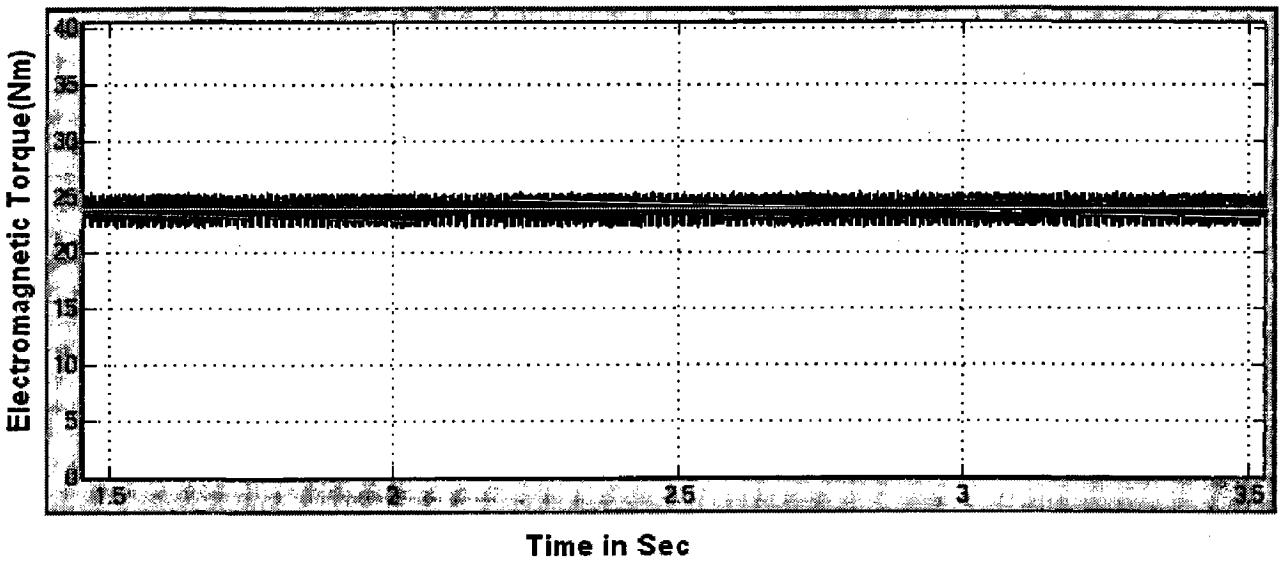

5.12(b) Electromagnetic torque with respect to time in Fuzzy DTC

Fig 5.12a shows the electromagnetic torque with respect to time. for classical DTC. Figure 5.11(b) shows of the electromagnetic torque for the DTC using fuzzy based SVM. From the comparison Fig5.12 (a) and (b), it can be observed that fuzzy based SVM has less torque ripples.

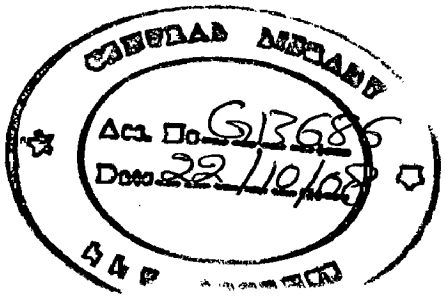

Chapter-6

CONCLUSIONS AND FUTURE SCOPE

6.1 Conclusions

Vector Control and Direct Torque Control have been widely used for dynamic torque and flux control of AC machines. Both methods have their own advantages and disadvantages. The FOC needs co-ordinate transformations. Because of these co-ordinate transformations the precision of the control strategy depends on machine parameters and the dynamic response also depends on the method of current control. On the other hand DTC has the advantage of being more robust to change in parameters and free from co-ordinate transformations. However, it has the disadvantage of having high ripples in torque and flux as nonlinear hysteresis controllers are used for torque and flux control. This disadvantage can be overcome by using fuzzy space vector modulation technique.

The performance of the classical DTC Induction motor drive has been improved with the FSVM. From the simulation study, it has been observed that the DTC of Induction motor using fuzzy based SVM has less torque ripples and reduced flux error.

6.1 Future Scope

In this thesis, performance of the DTC based induction motor drive using Fuzzy SVM was investigated using 2-level inverter. This can be extended to multi level inverters for better performance.

REFERENCES

[1]. I. Takahashi and T. Noguchi, "A new quick response and high efficiency strategy of an induction motor," in *Conf. Rec. IEEE-IAS Annu. Meeting*, 1985, pp. 495–502.

[2]. M. Depenbrock, "Direct-self control of inverter-fed induction machine,"*IEEE Trans. Power Electrons*, Vol. 3, no. 4, pp. 420–429, 1988.

[3]. aI. Takahashi and Y. Ohmori, "High-performance direct torque control of induction motor," *IEEE Trans. Ind. Appl.*, Vol. 25, no. 2, pp. 257–264, 1989.

[4]. T. G. Habetler, F. Profumo, M. Pastorelli, and L. M. Tolbert, "Direct torque control of induction machines using space vector modulation," *IEEE Trans. Ind. Appl.*, Vol. 28, no. 5, pp. 1045–1053, 1992.

[5]. D. Casadei, G. Grandi, G. Serra, and A. Tani, "Effects of Flux and Torque Hysteresis Band Amplitude in Direct Torque Control of Induction Machines," Industrial Electronics, Control and Instrumentation, 1994. IECON '94, 20th International Conference, pp. 299–304.

[6]. Nik Rumzi Nik Idris, *and* Abdul Halim Mohamed Yatim, "Direct Torque Control of Induction Machines With Constant Switching Frequency and Reduced Torque Ripple", *IEEE Trans. Ind. electronics.*, Vol. 51, no. 4, pp. 758–767, 2004

[7]. Peter Vas, "Sensorless Vector and Direct Torque Control", Oxford University Press, 1998.

[8]. B.K Bose, "Modern Power Electronics and AC Drives", Prentice Hall PTR, 2002.

[9]. R.Krishnan, "Electric Motor Drives-modeling, analysis, and control", Prentice Hall of India, private limited.

[10]. S.Chakrabarthi, M.Ramamoorty and V.R Kanetkar, "Reduction Of Torque Ripple In Direct Torque Control Of Induction Motor Drives Using Space Vector Modulation" - Power Electronics and Drive Systems, 1997. Proceedings, 1997 International Conference.

[11]. Lin Chen, Kang-Ling Fang, and Zi-fan hu," A Scheme of Fuzzy Direct Torque Control for induction motor", Proceedings of the Fourth International Conference on Machine Learning and Cybernetics, Guangzhou, 18-21 August 2005

[12]. Tripathi, A. M. Khambadkone, and S. K. Panda, "Space-vector based, constant frequency, direct torque control and dead beat stator flux control of ac machines,"

in *Proc. IEEE Int. Conf. Industrial Electronics, Control, Instrumentation Automation (IECON'01)*, vol. 2, Nov. 2001, pp. 1219–1224.

[13]. T. Noguchi, M. Yamamoto, S. Kondo, and I. Takashi, "High frequency switching operation of PWM inverter for direct torque control of induction motor," in *Conference Record IEEE IAS Annual Meeting*, 1997, pp. 775–780.

[14]. M. P. Kazmierkowski and A. B. Kasprowicz, "Improved direct torque and flux vector control of PWM inverter-fed induction motor drives," *IEEE Trans. Ind. Electron.*, vol. 42, no. 4, pp. 344–349, 1995.

[15]. G. Buja, D. Casadei, and G. Serra, "Direct stator flux and torque control of an induction motor: Theoretical analysis and experimental results," in *Proceedings of the IECON '98*, vol. 1, 1998, pp. T50–T64.

[16]. X. Xu, R. DeDoncker, and D. W. Novotny, "A stator flux oriented induction machine drive," in *PESC I988 Conf Rec.*, pp. 870-876.

[17]. Yen-Shin Lai, Member, and Jian-Ho Chen," A New Approach to Direct Torque Control of Induction Motor Drives for Constant Inverter Switching Frequency and Torque Ripple Reduction", *IEEE Trans* on energy conversion., vol. 16, no. 3, pp. 220–227, 2001.

[18]. J. Holtz, "Pulse width modulation—a survey," *IEEE Trans. Ind. Electron.*, vol. 38, no. 5, pp. 410–420, Oct. 1992.

[19]. J. Holtz, W Lotzkat, and A. M. Khambadkone, "On continuous control of pwm inverters in overmodulation range including the six step-mode," *IEEE Transaction on Power Electronics,* vol. 8, no. 4, pp. 546-553, 1993.

[20]. P. G. Handley and J. T. Boys, "Practical real-time pwm modulators: An assessment," *Proc. Inst. Elect. Eng. B*, vol. 139, no. 2, pp. 96–102, Mar. 1992.

[21]. P. Marino, M. D'Incecco and N.Visciano "A Comparison of Direct Torque Control Methodologies for induction Motor" 2001 IEEE

[22]. Arias; J.L. Romeral, E. Aldabas "Fuzzy Logic Direct Torque Control" 2000 IEEE

[23]. "Novel Direct Torque Control (DTC) Scheme With Fuzzy Adaptive Torque-Ripple Reduction" Luis Romeral, Antoni Arias, Emiliano Aldabas members IEEE, and Marcel.G.Jayne IEEE TRANSACTIONS ON INDUSTRIAL ELECTRONICS, VOL. 50, NO. 3, JUNE 2003.

[24]. M. Depenbrock, "Pulse width control of a three phase inverter with nonsinusoidal phase voltages," in *Proc. IEEE-ISPC Conference*, 1977, pp. 399–403.

[25]. D. Rathnakumar, J LakshmanaPerumal, T. Srinivasan, "A new software implementation of space vector PWM," in *IEEE Proceedings,* pp. 131 – 136, April 2005.

[26]. D. Jenni and F. Wueest, "The optimization parameters of space vector modulation," in *Proc. 5th European Conf. Power Electronics and Applications*, pp. 376–381, 1993.

[27]. S. R. Bowes and Y. S. Lai, "The relationship between space vector modulation and regular-sampled PWM," *IEEE Trans. Power Electron.*, vol.14, pp. 670–679, Sept. 1997.

[28]. Zhou and D. Wang, "Relationship between space-vector modulation and three-phase carrier-based PWM: A comprehensive analysis," *IEEE Trans. Ind. Electron.*, vol. 49, pp.186–196, Feb. 2002.

[29]. V.R Stefanovic,. S.N Vukosavic, "Space-vector PWM voltage control with optimized switching strategy," *IEEE Industry Appl. Society Annual Meeting, 1992., Conference Record*, vol.1 pp.1025 – 1033, Oct. 1992

[30]. H.W. van der Broeck, H.C.Skudelny, G.V. Stanke: "Analyses and Realization of a Pulsewidth Modulator Based on Voltage Space Vectors" , *IEEE Trans. Ind. Appl*, vol. IA-24, No. 1, pp 142-150, Jan/Feb.1988.

APPENDIX

List of motor specification and parameters

5 HP,400 V, 3 phase, 50Hz,4 poles,

Motor Parameters

Stator Resistance, Rs = 4.68 ohm

Rotor Resistance, Rr = 5.06 ohm

Stator self Inductance, Ls = 0.0039 H

Rotor self Inductance, Lr = 55.1 mH

Mutual Inductance, Lm = 0.93 H